

Testing the Concept of Quark-Hadron Duality with the ALEPH τ Decay Data

B.A. Magradze

Received: date / Accepted: date

Abstract We propose a modified procedure for extracting the numerical value for the strong coupling constant α_s from the τ lepton hadronic decay rate into non-strange particles in the vector channel. We employ the concept of the quark-hadron duality specifically, introducing a boundary energy squared $s_p > 0$, the onset of the perturbative QCD continuum in Minkowski space [1, 2, 3]. To approximate the hadronic spectral function in the region $s > s_p$, we use contour improved perturbation theory (CIPT) up to the fifth order. A new feature of our procedure is that it enables us to extract from the data simultaneously the QCD scale parameter $\Lambda_{\overline{\text{MS}}}$ and the boundary energy squared s_p . We carefully determine the experimental errors on these parameters which come from the errors on the invariant mass squared distribution. For the $\overline{\text{MS}}$ scheme coupling constant, we obtain $\alpha_s(m_\tau^2) = 0.3204 \pm 0.0159_{exp.}$. We show that our numerical analysis is much more stable against higher-order corrections compared to the standard one. Additionally, we recalculate the “experimental” Adler function in the infrared region using final ALEPH results. The uncertainty on this function is also determined.

Keywords tau lepton decay · renormalization group equation · perturbation theory data analysis

1 Introduction

The hadronic τ decays serves as an ideal laboratory for testing quantum chromodynamics (QCD) in a relatively low energy regime. In the past, various techniques (fixed order perturbation theory, contour improved perturbation theory, effective charge approach, renormalons, dispersive approach) have been devised to improve the reliability of the predictions of the theory for the τ system. In this boundary area of the energy, perturbative ideas are still applicable due to relatively large mass of the τ lepton, while non-perturbative effects are expected to be small. Usually, they are under control within Wilson Operator Product Expansion (OPE) [4]. It is known that the main

B.A. Magradze
Andrea Razmadze Mathematical Institute, M. Aleksidze St. 1, Tbilisi 0193, Georgia
E-mail: magr@rmi.acnet.ge

calculational tool in perturbative QCD (pQCD) the renormalization group improved perturbation theory augmented with the OPE can not be used locally in the time-like region even at high energy. Fortunately, this problem has been resolved in earlier work [5] by using the idea of the quark-hadron duality. The assumption is that the QCD perturbation theory may still be used in Minkowski region to describe some global (inclusive) quantities like τ lepton decay rate. Although the quark-hadron duality cannot be justified rigorously from the first principles, in practice this idea works good enough. On this basis, an accurate description of the τ lepton decay data was achieved (see the seminal work [6] and the literature therein). However, one should always keep in mind that the duality between a physical quantity and its quark-gluon perturbation theory representation is only approximative and thus it must inevitable be violated (see the review [7] and the literature therein). To identify general mechanism of Duality Violations (DVs), special QCD inspired models for the hadronic spectral functions (e.g. the instanton-based and resonance-based models [7] as well as the models motivated by the large N_c limit of the theory [8,9,10]) have been studied. In these models DVs in fact occur. Presumably, DVs arise due to the lack of the convergence of the OPE on the Minkowski axis. If this is the case, then the analytical continuation of the truncated OPE series from the Euclidean region to the physical axis is questionable [7,10].

On the other hand, in recent years, the accuracy of the measurements of the observables of the τ lepton system has been essentially improved (for the recent results of the ALEPH collaboration see [11,12,13,14]). This enables one to extract the parameters of the standard model from τ data with very high precision. Of particular interest is the numerical value of the strong coupling constant α_s . Admittedly, one of the most precise determinations of the strong coupling constant comes from the analysis of the τ data (for most recent results see [14]). An independent low-energy highest-precision determination of α_s comes from lattice QCD simulations combined with experimental data for hadron masses [15]. These two highest-precision determinations extrapolated to the Z mass yield

$$\alpha_s(M_z^2) = 0.1212 \pm 0.0011 \quad (\tau \text{ decay}) \quad (1)$$

$$\alpha_s(M_z^2) = 0.1170 \pm 0.0012 \quad (\text{lattice}). \quad (2)$$

Note that the agreement between these two results, with the errors quoted, is not good. They differ from each other by about 2.6 standard deviations. Furthermore, the lattice determination is closer to $\alpha_s(M_z^2)$ values obtained from high energy experiments. Thus, the reliability of the estimates from the τ -lepton data has been called in question [9, 10, 14, 16].

To estimate systematic effects from DVs, recently the authors of [14] have analyzed the ALEPH τ data for the V+A spectral function using two different models for the spectral function. These models were previously considered in [7,9]. It was confirmed that DVs effects in this channel within these models are completely negligible. However, this result has been reanalyzed in [10]. There the vector (V) and axial-vector (A) spectral functions have separately been considered. To describe DVs coming from the region $s \geq 1.1 \text{ GeV}^2$ physically motivated models for these spectral functions have been suggested. Analyzing the τ data provided by the ALEPH collaboration, the authors of [10] have concluded that DVs are not small. An additional systematic error in the value of the coupling constant coming from DVs has been estimated on the level $\delta\alpha_s(m_\tau^2) \approx 0.003 - 0.010$.

As is well known, in the time-like region the renormalization group (RG) invariance cannot be used unambiguously. Usually, the QCD corrections to the τ lepton decay

rate R_τ is expressed via the contour integral of the associated Adler function multiplied by the known weight function. This representation is valid owing to special analyticity structure of the corresponding exact current-current correlation function. The Adler function is represented via the truncated perturbation theory series and the integral is taken over the circle of radius m_τ^2 (m_τ stands for the τ -lepton mass) in the complex energy squared plane [6]. One possibility is to integrate term-by-term the truncated perturbation theory series over the contour and then perform the RG improvement. This approach is referred to as fixed order perturbation theory (FOPT). Alternatively, one can insert the RG improved truncated series for the Adler function inside the contour integral and then perform the integral. This approach suggested in [17, 18, 19] was termed contour improved perturbation theory (CIPT). The advantage of CIPT is that it enables to resume some higher-order contributions to the rate. These two approaches lead to differing results. The values of α_s extracted from τ decays employing CIPT have always been higher. A detailed comparison of these two approaches may be found in recent works [20, 21]. A practical review of various approaches to the τ decay rate may be found in [13].

The inclusive quantity like hadronic τ decay rate may be accurately described within pure perturbative approach, provided the DVs are small. Indeed, the nonperturbative power suppressed contributions described by the OPE (continued analytically to the time-like region) have been estimated to be small [6]. However, the large value of the running coupling parameter at the τ lepton mass scale leads to the large renormalization scheme dependence of perturbative predictions. To reduce this dependence various resummation techniques have been developed (see, for example, [22, 23, 24]). In [22], to determine more accurately the value for the coupling constant from the τ -lepton data a modified extraction procedure (based on the effective charge approach) has been employed. The numerical analysis has been performed in the internal renormalization scheme of the τ system and then the result was translated into the $\overline{\text{MS}}$ scheme using renormalization scheme transformation. This procedure yields smaller value for the coupling constant. Similarly, in [23] and [24] in calculations of the τ decay rate the minimal sensitivity and effective charge schemes were used. In this way the reliability of the estimates for the coupling constant has been improved.

A serious shortcoming of the conventional perturbation theory approximations to the current-current correlation functions parameterized in terms of the running coupling is that they do not obey correct analytical properties of the corresponding exact quantities. The analytical properties are violated due to the non-physical Landau singularities of the perturbative running coupling which occur at small space-like momenta (for the analytical structure of the perturbative coupling beyond the one loop order see [25, 26, 27, 28]). Supposedly, these singularities may deteriorate the extracted values of the parameters [29]. On the other hand, this shortcoming may be avoided by using dispersive or analytic approaches to pQCD. At present, several such approaches are being intensively developed [30, 31, 32, 33, 34, 35, 36, 37, 38, 39, 40, 41]. In [33], the τ lepton decay rate has been analyzed within a simple and effective dispersive technique, the Analytic Perturbation Theory (APT) (for reviews see [34, 35, 36, 41]). The advantages and shortcomings of the three approaches to the τ decays (FOPT, CIPT and APT) were thoroughly analyzed in [37]. It should be noted that the APT as well as its generalized versions suggested more later [40] proved to be very useful from the phenomenological point of view. A remarkable feature of these modified expansions is the better convergence and improved stability property with respect to change of the renormalization scheme. Nevertheless, one should keep in mind that an analytic

approach based only on perturbation theory can not be defined unambiguously, since there is not a unique recipe for removing the Landau singularities from the running coupling.

A particular problem emerges from the observation that the QCD perturbation theory augmented with the OPE fail to describe the detailed infrared behavior of the Adler function associated with the τ decay rate [3]. To treat this problem a more general framework is required. A suitable theoretical framework was suggested in [3]. There the hadronic non-strange vector spectral function $v_1(s)$ ¹ was approximated by a simple *ansatz*

$$v_1(s) \approx \theta(s_p - s)v_1^{np.}(s) + \theta(s - s_p)v_1^{pQCD}(s), \quad (3)$$

where $v_1^{pQCD}(s)$ is the perturbation theory approximation to the spectral function and s_p is the onset of perturbative continuum², an infrared boundary in Minkowski region above which we trust pQCD. The non-perturbative component of the spectral function $v_1^{np.}(s)$ was described by a resonance based model (“the lowest meson dominance approximation to large- N_c QCD”). Using this model the authors of [3] have achieved correct matching in the intermediate region between the pQCD and Chiral Perturbation Theory predictions for the Adler function³. To compare the Adler function evaluated from (3) to the experiment the authors of [3] have also constructed the “experimental” spectral function

$$v_1^{\text{“exp.”}}(s) = \theta(s_p - s)v_1^{exp.}(s) + \theta(s - s_p)v_1^{pQCD}(s), \quad (4)$$

where $v_1^{exp.}(s)$ is the genuine experimental part of the total “experimental” spectral function which is measured with high precision by ALEPH [11,42] and OPAL [43] collaborations in the range $0 < \sqrt{s} < m_\tau = 1.777 \text{ GeV}$. Formula (4) extends the spectral function beyond the range accessible in the experiment. Formula (3) or (4) can be treated as a practical realization of the concept of the quark-hadron duality (see the original works [1,2]). In this formulation of the duality one does not rely on the procedure of the analytical continuation of the truncated OPE to Minkowski region—a source of the possible DVs. The conventional formulation of the duality may be recovered from formulas (3) or (4) by taking the limit $s_p \rightarrow 0$ and introducing the OPE contributions. Note that, model (3) describes only such non-perturbative corrections to the spectral function which are essentially confined in the low energy region $0 < s < s_p$.

In this paper we concentrate on formula (4). Our aim is to utilize the total information encoded in this representation. We recall that the authors of [3] have used *ansatz* (4) to extract the numerical value for the parameter s_p from the experimental data. For the $\overline{\text{MS}}$ scheme scale parameter (for the three active flavours) they have used the estimate

$$\Lambda_{\overline{\text{MS}}} = (372 \pm 72) \text{ MeV}. \quad (5)$$

The QCD component of the spectral function, $v_1^{pQCD}(s)$, was determined from the order $\mathcal{O}(\alpha_s^3)$ approximation to the Adler function, while the exact numeric two-loop

¹ We use the normalization of the spectral function with the naive parton prediction $v_{1,naive} = 1/2$.

² It is assumed that the inequality $0 < s_p < m_\tau^2$ holds.

³ The infrared behaviour of the Adler function was also correctly described within APT [38]. However, APT requires large effective quark masses to reproduce the τ data.

running coupling constant, normalized at the scale s_p , was employed. The experimental component $v_1^{exp.}(s)$ has been reconstructed from the ALEPH collaboration data obtained in 1999 [42]. Note that the estimate (5) is close to the ALEPH result for the scale parameter obtained for that time

$$\Lambda_{\overline{\text{MS}}} = (370 \pm 51) \text{ MeV}.$$

However, direct comparison of these two results will not be wholly correct. The final result of the collaboration for the coupling constant corresponds to the average of the two values obtained within the FOPT and CIPT approaches, while in [3] only FOPT was used. Furthermore, in the ALEPH analysis the estimate for $\mathcal{O}(\alpha_s^4)$ term have also been included, while the QCD scale parameter was extracted using the exact (numeric) four loop running coupling. Using the *ansatz* (4) the authors of [3] have derived consistency condition from the OPE, an equation relating the parameters s_p and $\Lambda_{\overline{\text{MS}}}$. From this equation, with the estimate (5), they have found that

$$s_p = (1.60 \pm 0.17) \text{ GeV}^2. \quad (6)$$

Usually, it is more convenient to compare the time-like experimental data with theory via the Adler function, the object determined in the space-like region [44]⁴

$$D(Q^2) = Q^2 \int_0^\infty \frac{2v_1(s)ds}{(s+Q^2)^2}, \quad (7)$$

for this quantity reliable approximations are constructed in pQCD, in massless [45, 46, 47, 48, 49] as well as in massive cases [49, 44]. The “experimental” Adler function is obtained by inserting *ansatz* (4) into integral (7)

$$D_{\text{“exp.”}}(Q^2) = D_{exp.}(Q^2, s_p) + D_{pQCD}(Q^2, s_p), \quad (8)$$

where the experimental and perturbation theory components of the total “experimental” Adler function are defined as

$$D_{exp.}(Q^2, s_p) = Q^2 \int_0^{s_p} \frac{2v_1^{exp.}(s)ds}{(s+Q^2)^2}, \quad D_{pQCD}(Q^2, s_p) = Q^2 \int_{s_p}^\infty \frac{2v_1^{pQCD}(s)ds}{(s+Q^2)^2}. \quad (9)$$

Note that the “experimental” Adler function is not wholly experimental quantity, since it depends also on the theoretical component $D_{pQCD}(Q^2, s_p)$. The latter may be calculated using different theoretical approaches. For example, one may apply FOPT, CIPT or a dispersive approach. Furthermore, the result will depend on the higher order corrections to the β -function and to the Adler function. In the past years, the “experimental” Adler function was employed for testing various theoretical approximations to the Adler function [3, 38, 39].

In view of appearance of final ALEPH data in 2005 [11, 12] it is worthwhile to recalculate the “experimental” Adler function. In this paper we extend the analysis of work [3] in several directions. First, we will use different strategy for extracting numerical values of the parameters from the data. The distinguishing feature of our analysis is that we will determine both parameters ($\Lambda_{\overline{\text{MS}}}$ and s_p) self-consistently. Secondly, we pay particular attention to the estimation of the experimental errors on the parameters and Adler function. Furthermore, we choose the CIPT approach.

⁴ we use notation $q^2 = -Q^2$ and $Q^2 > 0$ for space-like momenta

In Sect. 2 we evaluate the perturbative component of the hadronic spectral function within the CIPT approach up to order $\mathcal{O}(\alpha_s^5)$. Then, we derive a transcendental system of equations for the parameters $\Lambda_{\overline{\text{MS}}}$ and s_p . The first equation of the system follows from the OPE for the current-current correlation function in the limit of massless quarks⁵. The second equation for the parameters is a consequence of the quark-hadron duality implemented by means of the *ansatz* (4): We use this *ansatz* to calculate the τ -lepton decay rate. In Sect. 3 we solve the system of equations for the parameters numerically. To determine the empirical contributions in the equations, we employ the final ALEPH data on the non-strange vector invariant mass squared distributions which are available in [12]. To test the stability of the numerical results against the QCD perturbative corrections, we use different approximations to the Adler function from order $\mathcal{O}(\alpha_s)$ to order $\mathcal{O}(\alpha_s^5)$. This enables us to determine the so-called indicative theoretical errors [22] on the extracted numerical values of the parameters. The statistical errors on the parameters are carefully estimated. Our approach, which we refer to as CIPT⁺, is compared with the standard CIPT. In the most of the calculations, we use the four loop running coupling. In Sect. 4, we present numerical results for the “experimental” Adler function obtained from the final ALEPH data. The values and associated experimental errors of the function are tabulated in the region $Q = 0 - 1.5$ GeV. Our conclusions are given in Sect. 5. In Appendix A we give some practical formulas obtained with the explicit (series) solution to the higher order RG equation. The errors are analyzed in detail in Appendix B. In Appendix C we present some required results obtained within standard CIPT.

2 Theoretical Framework

The main quantity of interest for following analysis is the Adler function associated with the vector current two-point correlator. The perturbative expansion of this function in the limit of vanishing quark masses reads [20]

$$D(Q^2) = \sum_{n=0}^{\infty} a_s^n(\mu^2) \sum_{k=1}^{n+1} k c_{n,k} L^{k-1} \quad \text{where} \quad L \equiv \ln \frac{Q^2}{\mu^2}, \quad (10)$$

$a_s(\mu^2) = \frac{\alpha_s(\mu^2)}{\pi}$ with $\alpha_s(\mu^2)$ being the strong coupling constant renormalized at the scale μ . Since the Adler function is a physical quantity, it satisfies a homogenous RG equation. This fact enables us to choose $\mu^2 = Q^2$. Then the expansion (10) may be reexpressed as an asymptotic expansion in powers of the running coupling $\alpha_s(Q^2)$

$$D(Q^2) = \sum_{k=0}^{\infty} d_k \left(\frac{\alpha_s(Q^2)}{\pi} \right)^k, \quad (11)$$

where $d_n = c_{n,1}$. The first two coefficients in series (11) are universal $d_0 = d_1 = 1$. The coefficients of order a_s^2 and a_s^3 in the $\overline{\text{MS}}$ scheme have been calculated about thirty and fifteen years ago [45, 46, 47]. Recently, the authors of [48] have calculated the coefficient d_4 in the case of massless quarks by using powerful computational techniques. The known higher order coefficients in the $\overline{\text{MS}}$ scheme for $n_f = 3$ quark flavours take values $d_2 \simeq 1.6398$, $d_3 \simeq 6.3710$ and $d_4 \simeq 49.0757$.

⁵ The FOPT version of this equation has been derived in [3].

In practice the series (11) should be truncated. The obtained approximations to the Adler function do not obey correct cut-plane analyticity properties of the exact function because of the unphysical “Landau singularities” which present in the perturbative running coupling. The exact Adler function $D(z)$ ($z = Q^2 = -q^2$) is known to be analytic except the cut running along the negative real axis. This fact enables us to calculate the hadronic non-strange vector spectral function from the Adler function via the contour integral

$$2v_1(s) = \frac{1}{2\pi i} \oint_{-s-i0}^{-s+i0} \frac{D(z)}{z} dz, \quad (12)$$

where the path of integration, connecting the points $-s \mp i0$ on the complex z -plane, avoids the cut running along the real negative axis. The integral being traversed in a positive (anticlockwise) sense. In this paper we shall assume, without loss of generality, that the approximation (11) to the Adler function has only one unphysical singularity located on the positive real axis. This is the case, for example, if we use the exact (explicitly solved) two-loop order running coupling in $\overline{\text{MS}}$ like renormalization schemes⁶. On the other hand, a running coupling at higher orders may be expanded in powers of the exact (explicitly solved) two-loop order coupling [50, 51]

$$\alpha_s^{(k-\text{loops})}(Q^2) = \sum_{n=1}^{\infty} C_n^{(k)} \alpha_s^{(2-\text{loops})n}(Q^2)|_{\text{exact}}, \quad (13)$$

where the numerical coefficients $C_n^{(k)}$ are determined in terms of the β -function coefficients (see Appendix A). It has been shown in [28] that this series has a sufficiently large radius of convergence in the space of the coupling constants, and its partial sums provide very accurate approximations to the exact k -th order ($k > 2$) coupling in the complex Q^2 plane. To construct accurate approximations to the running coupling for small values of $|Q|^2$, one should retain sufficiently large number of terms in the partial sum. In this approximation, the Adler function has an unphysical singularity located on the positive Q^2 -axis. The corresponding cut runs along the finite interval of the positive Q^2 -axis. Nevertheless, formula (12) is still valid provided that the integration contour avoids the physical and unphysical cuts.

Let us separate out the parton level term from the perturbative Adler function

$$D_{RGI}(Q^2) = 1 + d_{RGI}(Q^2) : \quad d_{RGI}(Q^2) = \sum_{k=1}^{\infty} d_k a_s^k(Q^2), \quad (14)$$

where $a_s(Q^2) = \frac{a_s(Q^2)}{\pi}$ and the subscript “RGI” refers to the renormalization group improved perturbation theory. As it was discussed above, the function $d_{RGI}(Q^2)$ is analytic except the cuts running along the real Q^2 -axis. The physical cut runs along the real negative interval $-\infty < Q^2 < 0$, and the unphysical cut runs along the positive interval $0 < Q^2 < s_L$, where the point $Q^2 = s_L > 0$ corresponds to the “Landau singularity”. We may then write a Cauchy relation

$$d_{RGI}(Q^2) = \frac{1}{2\pi i} \oint_{\Gamma} \frac{d_{RGI}(w)}{w - Q^2} dw \quad (15)$$

⁶ the analytic structure of the explicit exact solution to the RG equation at the two loop order has been determined in [25, 26, 27].

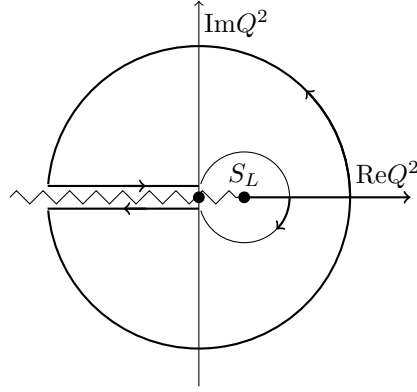


Fig. 1 Contour in the complex Q^2 plane used in the Cauchy relation (15). Branch points on the real axis are represented by the blobs and brunch cuts by the zigzagging line.

where the integral is taken round the closed contour Γ drawn in Fig.1. The contour consists of the arc of the circle $|Q^2 - s_L| = s_L$, straight lines parallel to the real negative Q^2 axis and passes round a big circle. Using formula (15) together with the asymptotic condition $d_{RGI}(z) \rightarrow 0$ as $|z| \rightarrow \infty$, we derive a violated dispersion relation (DR) for the function $d_{RGI}(Q^2)$. Hence we may write

$$d_{RGI}(Q^2) = d_{APT}(Q^2) + d_L(Q^2) \quad (16)$$

where the function $d_{APT}(Q^2)$ satisfies the normal DR

$$d_{APT}(Q^2) = \frac{1}{\pi} \int_0^\infty \frac{\rho_{eff}(\sigma)}{\sigma + Q^2} d\sigma, \quad (17)$$

with the effective spectral density

$$\rho_{eff}(\sigma) = \text{Im}\{d_{RGI}(-\sigma - i0)\}. \quad (18)$$

It is to be noted here that the function

$$D_{APT}(Q^2) = 1 + d_{APT}(Q^2) \quad (19)$$

is the analytic image of the perturbative Adler function determined in the sense of the Analytic Perturbation Theory (APT) approach of Shirkov and Solovtsov [34,35]. The second term in (16), which violates the DR, corresponds to the contribution to the integral (15) coming from the “Landau branch cut”. It is represented by the contour integral

$$d_L(Q^2) = -\frac{1}{2\pi i} \oint_{C_L^+} \frac{d_{RGI}(\zeta)}{\zeta - Q^2} d\zeta, \quad (20)$$

taken round the circle $\{\zeta : \zeta = s_L + s_L \exp(i\phi), -\pi < \phi \leq \pi\}$ in the positive (anti-clockwise) direction.

The perturbation theory approximation to the hadronic spectral function is calculated by inserting the series (14) into the inversion formula (12). An important point

is that the “Landau part” $d_L(Q^2)$ does not contribute into the spectral function, provided that $s > 0$. To see this, let us rewrite this contribution to the spectral function, with the aid of formula (20), as follows

$$2v_1(s)|_L = \frac{1}{2\pi i} \oint_{-s-i0}^{-s+i0} \frac{d_L(z)}{z} dz = - \left(\frac{1}{2\pi i} \right)^2 \oint_{-s-i0}^{-s+i0} \frac{dz}{z} \oint_{C_L^+} \frac{d_{RGI}(\zeta)}{\zeta - z} d\zeta = \\ - \frac{1}{2\pi i} \oint_{C_L^+} d\zeta d_{RGI}(\zeta) \left\{ \frac{1}{2\pi i} \oint_{-s-i0}^{-s+i0} \frac{1}{z(\zeta - z)} dz \right\}, \quad (21)$$

here we have interchanged the order of integration in the repeated integral. Let us consider the integral under braces. For $\zeta \neq 0$ the integrand has two simple poles inside the contour of integration. It is evident that this integral vanishes by the theorem of residues, provided $s > 0$,

$$\frac{1}{2\pi i} \oint_{-s-i0}^{-s+i0} \frac{1}{z(\zeta - z)} dz \equiv 0,$$

and the same result holds for $\zeta = 0$. We have thus found that only the “analytic component” $d_{APT}(Q^2)$ has a finite contribution into the hadronic spectral function. Insert the DR (17) into the inversion formula (12) and interchange the order of integration

$$2v_1^{CI}(s) = \frac{1}{2\pi i} \oint_{s-i0}^{s+i0} (1 + d_{APT}(z)) \frac{dz}{z} = \\ 1 + \frac{1}{\pi} \int_0^\infty d\sigma \rho_{eff}(\sigma) \left\{ \frac{1}{2\pi i} \oint_{-s-i0}^{-s+i0} \frac{dz}{z(z + \sigma)} \right\}, \quad (22)$$

the superscript “CI” in the function $v_1^{CI}(s)$ refers to the contour improved perturbation theory. The integral under braces on the second line of (22) is calculated by using the theorem of residues. We then find the relation

$$2v_1^{CI}(s) = 1 + \frac{1}{\pi} \int_s^\infty \frac{\rho_{eff}(\sigma)}{\sigma} d\sigma. \quad (23)$$

With the help of formula (23), we express the “perturbative component” of the total “experimental” Adler function in terms of the effective spectral density

$$D_{CI}(Q^2, s_p) = \int_{s_p}^\infty \mathcal{K}(Q^2, s) 2v_1^{CI}(s) ds = \int_{s_p}^\infty \mathcal{K}(Q^2, s) (1 + r(s)) ds \quad (24)$$

where we have introduced the notations $D_{CI}(Q^2, s_p) \equiv D_{pQCD}(Q^2, s_p)$, $\mathcal{K}(Q^2, s) = Q^2/(s + Q^2)^2$ and

$$r(s) = \frac{1}{\pi} \int_s^\infty \frac{\rho_{eff}(\sigma)}{\sigma} d\sigma. \quad (25)$$

Integrating (24) by parts we obtain a more convenient representation

$$D_{CI}(Q^2, s_p) = \frac{Q^2}{s_p + Q^2} (1 + r(s_p)) - \frac{Q^2}{\pi} \int_{s_p}^\infty \frac{\rho_{eff}(s)}{s(s + Q^2)} ds. \quad (26)$$

Let us now evaluate power suppressed corrections to the total “experimental” Adler function (8). We may rewrite the perturbative component of the Adler function identically

$$\begin{aligned} D_{CI}(Q^2, s_p) &= D_{APT}(Q^2) - \int_0^{s_p} \mathcal{K}(Q^2, s) 2v_1^{CI}(s) ds \\ &= D_{RGI}(Q^2) - d_L(Q^2) - \int_0^{s_p} \mathcal{K}(Q^2, s) 2v_1^{CI}(s) ds, \end{aligned} \quad (27)$$

in the first line of (27) we have used the definition of the analytic image of the Adler function

$$D_{APT}(Q^2) = 1 + d_{APT}(Q^2) = \int_0^\infty \mathcal{K}(Q^2, s) 2v_1^{CI}(s) ds, \quad (28)$$

which is easily deduced from the discussion given above formula (22). The last equality on the right of (27) follows from formula (16). The power suppressed part of the total “experimental” Adler function is determined as

$$D_{p.s.}(Q^2, s_p) = D_{\text{“exp.”}}(Q^2) - D_{RGI}(Q^2). \quad (29)$$

Combining formulas (8), (16) and (27), we rewrite formula (29) in the form

$$\begin{aligned} D_{p.s.}(Q^2, s_p) &= D_{\text{exp.}}(Q^2, s_p) + D_{CI}(Q^2, s_p) - D_{RGI}(Q^2) \\ &= \int_0^{s_p} \mathcal{K}(Q^2, s) 2v_1^{\text{exp.}}(s) ds - d_L(Q^2) - \int_0^{s_p} \mathcal{K}(Q^2, s) 2v_1^{CI}(s) ds. \end{aligned} \quad (30)$$

From definitions (20) and (24), we obtain the asymptotic formulas

$$\mathcal{K}(Q^2, s) \approx Q^{-2} + \mathcal{O}(sQ^{-4}), \quad d_L(Q^2) \approx c_L \Lambda^2 Q^{-2} + \mathcal{O}(\Lambda^4 Q^{-4}) \quad \text{as } Q^2 \rightarrow \infty \quad (31)$$

where the coefficient c_L is a pure number independent of Λ

$$c_L = \Lambda^{-2} \frac{1}{2\pi i} \oint_{C_L^+} d_{RGI}(\zeta) d\zeta. \quad (32)$$

Using formulas (30) and (31), we evaluate asymptotic expansion for $D_{p.s.}(Q^2, s_p)$. It follows from the OPE that the leading term proportional to Q^{-2} in the asymptotic expansion should be suppressed provided that the quarks are massless. This condition leads to the equation ⁷

$$0.5c_L \Lambda^2 + \int_0^{s_p} v_1^{CI}(s) ds = \int_0^{s_p} v_1^{\text{exp.}}(s) ds. \quad (33)$$

We now express the left side of Eq. (33) in terms of the effective spectral density using formula (23). By integrating by parts we obtain then

$$s_p(1 + r(s_p)) + \frac{1}{\pi} \int_0^{s_p} \rho_{\text{eff}}(\sigma) d\sigma + c_L \Lambda^2 = \int_0^{s_p} 2v_1^{\text{exp.}}(s) ds. \quad (34)$$

The coefficient c_L is calculated numerically from formula (32). In this calculation we use the exact (explicit) two loop running coupling and also exact (numeric) four loop running coupling ⁸. The results are

$$c_L^{2\text{-loop}} = 0.421163, \quad c_L^{4\text{-loop}} = 0.555401. \quad (35)$$

⁷ The FOPT version of this equation takes the form $\int_0^{s_p} v_1^{FO}(s) ds = \int_0^{s_p} v_1^{\text{exp.}}(s) ds$ (see [3]).

⁸ Application of the explicit series solution (13) yield the same result.

We now turn to the calculation of the normalized τ -lepton decay rate into non-strange hadrons in the vector channel

$$R_{\tau,V} = 6|V_{ud}|^2 S_{EW} \int_0^{m_\tau^2} w_\tau(s) v_1(s) ds : \quad w_\tau(s) = \frac{1}{m_\tau^2} \left(1 - \frac{s}{m_\tau^2}\right)^2 \left(1 + 2\frac{s}{m_\tau^2}\right), \quad (36)$$

where V_{ud} and S_{EW} denote the flavor mixing matrix element and an electro-weak correction term respectively [6]. Insert the mixed representation (4) for the spectral function into (36). The requirement that (4) describes the experimental value of $R_{\tau,V}$ leads to the equation

$$\int_0^{m_\tau^2} w_\tau(s) v_1^{\text{"exp"}}(s) ds = \int_0^{m_\tau^2} w_\tau(s) v_1^{\text{exp.}}(s) ds,$$

which may be rewritten as

$$\int_{s_p}^{m_\tau^2} w_\tau(s) v_1^{CI}(s) ds = \int_{s_p}^{m_\tau^2} w_\tau(s) v_1^{\text{exp.}}(s) ds. \quad (37)$$

Using the relation (23), we express the left hand side of (37) in terms of the effective spectral density. By integrating by parts, after some algebra, we obtain

$$\begin{aligned} \int_{s_p}^{m_\tau^2} w_\tau(s) v_1^{CI}(s) ds &= \frac{1}{4} \left(1 - \frac{s_p}{m_\tau^2}\right)^3 \left(1 + \frac{s_p}{m_\tau^2}\right) (1 + r(s_p)) \\ &\quad - \frac{1}{4\pi} \int_{s_p}^{m_\tau^2} \frac{\rho_{eff}(s)}{s} \left(1 - \frac{s}{m_\tau^2}\right)^3 \left(1 + \frac{s}{m_\tau^2}\right) ds. \end{aligned} \quad (38)$$

3 Numerical Results for the Parameters

To extract the parameters s_p and Λ from the data we have to solve the system of equations

$$\Phi_1(s_p, \Lambda^2) = \int_0^{s_p} v_1^{\text{exp.}}(s) ds, \quad (39)$$

$$\Phi_2(s_p, \Lambda^2) = \int_{s_p}^{m_\tau^2} w_\tau(s) v_1^{\text{exp.}}(s) ds, \quad (40)$$

where the functions $\Phi_{1,2}$ are defined as

$$\Phi_1(s_p, \Lambda^2) = \frac{s_p}{2} (1 + r(s_p)) + \frac{1}{2\pi} \int_0^{s_p} \rho_{eff}(\sigma) d\sigma + \frac{c_L}{2} \Lambda^2, \quad (41)$$

$$\begin{aligned} \Phi_2(s_p, \Lambda^2) &= (1 - \bar{s}_p)^3 (1 + \bar{s}_p) \frac{(1 + r(s_p))}{4} \\ &\quad - \frac{1}{4\pi} \int_{s_p}^{m_\tau^2} \frac{\rho_{eff}(s)}{s} (1 - \bar{s})^3 (1 + \bar{s}) ds, \end{aligned} \quad (42)$$

with $\bar{s}_p = s_p/m_\tau^2$ and $\bar{s} = s/m_\tau^2$. The right hand sides of Eqs. (39)-(40) are determined in terms of the empirical function $v_1^{\text{exp.}}(s)$. We reconstruct the experimental vector spectral function from the ALEPH 2005 spectral data for the vector invariant mass

Table 1 The first solution for the parameters s_p and $\Lambda = \Lambda_{\overline{\text{MS}}}$ obtained at N²LO. The two- and four-loop running couplings have been used. The extracted values of the strong coupling constant $\alpha_s(m_\tau^2)$ are also given. The error bars refer to the experimental uncertainty only.

Observable	Approximation to the β -function	
	Two-loop	Four-loop
s_p GeV ²	1.7112 ± 0.0539	1.7087 ± 0.0539
Λ GeV	0.3826 ± 0.0337	0.3483 ± 0.0297
$\alpha_s(m_\tau^2)$	0.3197 ± 0.0152	0.3214 ± 0.0158

squared distribution which is publicly available [12] (see Appendix B). To interpolate the spectral function between the measured (at discrete points) values, we use cubic splines.

We solve the system of equations (39)-(40) numerically using various approximations to the Adler function. Since the system is transcendental it has more than one solution. In Table 1, we present the first reasonable solution for the parameters obtained at next-to-next-to-leading order (N²LO)⁹. From the Table, we see that the predictions for s_p are stable with respect to the loop corrections to the β -function. In this regard, the QCD scale parameter is more sensitive. The two values of Λ obtained with the two- and four loop β -functions differ in about 10%. However, this corresponds to the small difference $\alpha_s(m_\tau^2)|_{4\text{-loop}} - \alpha_s(m_\tau^2)|_{2\text{-loop}} \approx 0.0017$.

The solution for s_p obtained with the two-loop running coupling should be compared with the estimate $s_p = 1.60 \pm 0.17$ extracted in [3] from the earlier ALEPH data. Our prediction for the central value of s_p (see Table 1) is greater in about 7%. However, with the more accurate data, we have obtained smaller experimental errors on the parameters (see Appendix B). Our estimate for the central value, $\Lambda_{2\text{-loop}} = 383$ MeV is somewhat above the value $\Lambda_{2\text{-loop}} = 372$ MeV accepted in [3]. However, one should keep in mind that in [3] only one equation, the FOPT counterpart of Eq. (39), has been utilized.

Note that the system (39)-(40) permits one more solution for the parameters in the range $200 \text{ MeV} < \Lambda < 600 \text{ MeV}$ (see Table 2). An attractive feature of this solution is that it predicts a smaller value for the onset of perturbation theory: $s_p = 0.607 \text{ GeV}^2 \approx m_\rho^2$ (m_ρ stands for the ρ -meson mass). However, considering current status of α_s we find the extracted value for the strong coupling constant too large. For this reason, we decline this solution.

We also determine the experimental uncertainties on the parameters coming from the uncertainties of the vector invariant mass squared distribution. The correlations between the errors of the distribution are properly taken into account. Cumbersome technical details of the error analysis are relegated into Appendix B.

It is useful to determine the so-called indicative estimates of the theoretical uncertainties on the numerical values of the parameters (for the definition see [22]). This requires us to test convergence of the numerical results order-by order in perturbation theory. We use consecutive approximations to the Adler function from LO to N⁴LO. For the unknown $\mathcal{O}(\alpha_s^5)$ correction, we use the geometric estimate $d_5 = d_4(d_4/d_3) = 378 \pm 378$ [14]. The results for the extracted values of the parameters are presented in Table 3. Formally, we may write a series for the numerical value of the coupling

⁹ we will use the abbreviation N^kLO to denote the order $\mathcal{O}(\alpha_s^{k+1})$ approximation to the Adler function.

Table 2 The same as in Table 1 for the case of the second solution for the parameters.

Observable	Approximation to the β -function	
	Two-loop	Four-loop
$s_p \text{ GeV}^2$	0.606 ± 0.003	0.607 ± 0.003
$\Lambda \text{ GeV}$	0.583 ± 0.018	0.522 ± 0.016
$\alpha_s(m_\tau^2)$	0.417 ± 0.010	0.424 ± 0.011

Table 3 Numerical values for the parameters in the $\overline{\text{MS}}$ scheme extracted from the τ data order-by-order within the modified procedure based on CIPT⁺.

Observable	Approximation to the Adler function				
	LO	NLO	N ² LO	N ³ LO	N ⁴ LO
$s_p \text{ GeV}^2$	1.6958	1.7063	1.7087	1.7097	1.7101
$\Lambda \text{ GeV}$	0.4047	0.3576	0.3483	0.3466	0.3473
$\alpha_s(m_\tau^2)$	0.3522	0.3263	0.3214	0.3205	0.3208

constant as follows

$$\alpha_s(m_\tau^2)|_{\text{N}^4\text{LO}} = \alpha_s(m_\tau^2)|_{\text{LO}} + \sum_{k=1}^4 \Delta_k,$$

where $\Delta_k = \alpha_s(m_\tau^2)|_{\text{N}^k\text{LO}} - \alpha_s(m_\tau^2)|_{\text{N}^{k-1}\text{LO}}$. Using the numbers listed in Table 3 (we use abbreviation CIPT⁺ for the modified CIPT accepted in this paper) we obtain the series

$$\alpha_s(m_\tau^2)|_{\text{N}^4\text{LO}}^{\text{CIPT}^+} = 0.3522 - 0.0259 - 0.0049 - 0.0009 + 0.0003. \quad (43)$$

The changes of the leading term induced by the consecutive corrections in the series are found to be: 7.35%, 1.39%, 0.26% and 0.09%. It is interesting to compare the series (43) with its counterpart obtained within standard CIPT. In Appendix C, we have analyzed the same data within standard CIPT. We obtain, within CIPT, the series

$$\alpha_s(m_\tau^2)|_{\text{N}^4\text{LO}}^{\text{CIPT}} = 0.485 - 0.095 - 0.023 - 0.013 - 0.007, \quad (44)$$

now the corrections provide more sizable changes of the leading term: 19.6%, 4.74%, 2.68% and 1.44%. The ratio $\Delta_k(\text{CIPT})/\Delta_k(\text{CIPT}^+)$ monotonically increases as a function of k from 3.7 at $k = 1$ to 23.3 at $k = 4$. Evidently, the series (43) converges more rapidly than the series (44). The indicative estimate of the theoretical uncertainty is determined as a half of the last retained term in the series [22]¹⁰. As pointed out in [22], the error defined in this way is heuristic and indicative. The actual values of the theoretical errors related to the uncalculated higher order terms in the perturbation theory series for the decay rate might be even large (see, for example, papers [6, 22, 23, 42]). In this paper, however, we shall consider only the indicative theoretical errors. From the series (43), we obtain the estimates

$$\begin{aligned} \alpha_s(m_\tau^2)|_{\text{NLO}} &= 0.3263 \pm 0.0159_{exp.} \pm 0.0130_{th} \\ \alpha_s(m_\tau^2)|_{\text{N}^2\text{LO}} &= 0.3214 \pm 0.0158_{exp.} \pm 0.0025_{th} \\ \alpha_s(m_\tau^2)|_{\text{N}^3\text{LO}} &= 0.3204 \pm 0.0159_{exp.} \pm 0.0005_{th} \\ \alpha_s(m_\tau^2)|_{\text{N}^4\text{LO}} &= 0.3208 \pm 0.0160_{exp.} \pm 0.0002_{th}, \end{aligned} \quad (45)$$

¹⁰ In [22] this definition of the uncertainty has been used within FOPT.

here we have also included the experimental errors. Analogically, from the CIPT series (44), one obtains

$$\begin{aligned}
\alpha_s(m_\tau^2)|_{\text{NLO}} &= 0.390 \pm 0.011_{exp.} \pm 0.048_{th} \\
\alpha_s(m_\tau^2)|_{\text{N}^2\text{LO}} &= 0.367 \pm 0.009_{exp.} \pm 0.012_{th} \\
\alpha_s(m_\tau^2)|_{\text{N}^3\text{LO}} &= 0.354 \pm 0.008_{exp.} \pm 0.007_{th} \\
\alpha_s(m_\tau^2)|_{\text{N}^4\text{LO}} &= 0.347 \pm 0.008_{exp.} \pm 0.004_{th},
\end{aligned} \tag{46}$$

here we have intentionally kept three decimal places, since the theoretical errors in this case are larger. The N^4LO estimates in (45) and (46) correspond to the central value $d_5 = 378$. The additional theoretical error induced from the uncertainty in the unknown coefficient d_5 takes the values 0.0002 and 0.0007 in the new and standard extraction procedures respectively. Comparing the numbers in formulas (45) and (46) we see that the indicative estimates of the theoretical error on the extracted numerical values of the coupling constant within the new procedure are considerable smaller. In contrast to this, the experimental errors on the values of α_s within the new procedure increases by the factor of 2. It is remarkable that a more reliable estimate of the theoretical error presented in [14] is close to the N^3LO and N^4LO values of the indicative error given in formula (46).

Similarly, determining the indicative theoretical errors on the parameter s_p , we find stable results

$$\begin{aligned}
s_p|_{\text{NLO}} &= 1.7063 \pm 0.0539_{exp} \pm 0.0525_{th} \\
s_p|_{\text{N}^2\text{LO}} &= 1.7087 \pm 0.0539_{exp} \pm 0.0012_{th} \\
s_p|_{\text{N}^3\text{LO}} &= 1.7097 \pm 0.0540_{exp} \pm 0.0006_{th} \\
s_p|_{\text{N}^4\text{LO}} &= 1.7101 \pm 0.0540_{exp} \pm 0.0002_{th},
\end{aligned} \tag{47}$$

Usually, it is convenient to perform evolution of the α_s results to the reference scale $M_z = 91.187 \text{ GeV}$. This is done by using RG equation and appropriate matching conditions at the heavy quark (charm and bottom) thresholds (see [52] and literature therein). The three loop level matching conditions in the $\overline{\text{MS}}$ scheme were derived in [53]. In this paper, we follow the work [54], where a very accurate analytic approximation to the four loop running coupling was suggested. We perform the matching at the matching scale $m_{th} = 2\mu_h$ where μ_h is a RG invariant mass of the heavy quark $\mu_h = \overline{m}_h(\mu_h)$. We assume for the RG invariant $\overline{\text{MS}}$ masses the values $\mu_c = 1.27^{+0.07}_{-0.11} \text{ GeV}$ and $\mu_b = 4.20^{+0.17}_{-0.07} \text{ GeV}$ [55]. Following [54], we evaluate the central value and error of $\alpha_s(M_z^2)$ using the formulas

$$\alpha_s(M_z^2) = (\alpha_s^+(M_z^2) + \alpha_s^-(M_z^2))/2 \quad \text{and} \quad \Delta\alpha_s(M_z^2) = (\alpha_s^+(M_z^2) - \alpha_s^-(M_z^2))/2$$

where $\alpha_s^\pm(M_z^2)$ denote the values obtained from $\alpha_s^\pm(m_\tau^2) = \alpha_s(m_\tau^2) \pm \Delta\alpha_s(m_\tau^2)$. In the evolution procedure, we have used the exact numeric four loop running coupling ¹¹. In Table 4, we compare the estimates for $\alpha_s(M_z^2)$ obtained within the new (CIPT⁺) and standard (CIPT) procedures. It is seen from the Table that the estimates obtained within CIPT⁺ at N^2LO , N^3LO and N^4LO orders practically coincide.

¹¹ We have confirmed that the approximate analytical coupling derived in [54] leads practically to the same numerical results.

Table 4 Estimates for $\alpha_s(M_z^2)$ obtained from the ALEPH τ lepton decay data order-by-order in perturbation theory. The results obtained within CIPT⁺ and CIPT are compared. Two errors are given, the experimental (first number) and the error from the evolution procedure (second number).

Approximation	$\alpha_s(M_z^2) _{\text{CIPT}^+}$	$\alpha_s(M_z^2) _{\text{CIPT}}$
N ² LO	$0.1187 \pm 0.0019 \pm 0.0005$	$0.1238 \pm 0.0009 \pm 0.0005$
N ³ LO	$0.1186 \pm 0.0019 \pm 0.0005$	$0.1224 \pm 0.0009 \pm 0.0005$
N ⁴ LO	$0.1186 \pm 0.0019 \pm 0.0005$	$0.1217 \pm 0.0009 \pm 0.0005$

Table 5 Comparison of the “experimental” Adler function $D_{\text{“exp.”}}(Q^2)$ and its QCD component $D_{CI}(Q^2, s_p)$ at low energies. The perturbative component is evaluated within the modified CIPT at N²LO using the four loop running coupling. The absolute and relative statistical errors of the “experimental” Adler function are tabulated.

Q GeV	$D_{\text{“exp.”}}(Q^2)$	$D_{CI}(Q^2, s_p)$	$\sigma(D_{\text{“exp.”}})$	rel.err.
0.1	0.0649	0.0063	0.0061	9.5%
0.2	0.2300	0.0249	0.0198	8.6%
0.3	0.4354	0.0545	0.0333	7.7%
0.4	0.6320	0.0933	0.0426	6.7%
0.5	0.7944	0.1391	0.0473	6.0%
0.6	0.9162	0.1895	0.0484	5.3%
0.7	1.0016	0.2426	0.0471	4.7%
0.8	1.0583	0.2965	0.0445	4.2%
0.9	1.0942	0.3497	0.0412	3.8%
1.0	1.1157	0.4013	0.0377	3.4%

4 Numerical Results for the “Experimental” Adler Function

Looking at the numbers in Table 1, we see that our estimates for the parameters are somewhat different than those used previously in [3]. Hence, it is sensible to recalculate the experimental Adler function in the infrared region. Another reason to do this is the appearance of the improved τ -data [12]. More importantly, it is desirable to carry out the error analysis too. Furthermore, in contrast to [3], in our calculations we will employ CIPT⁺.

The “experimental” Adler function and its QCD component are tabulated in Table 5. The QCD component of the “experimental” Adler function is calculated numerically at N²LO from formula (26). In the calculations we employ the four loop running coupling. For the parameters s_p and Λ , we use the values from Table 1. The absolute ($\pm 1\sigma$) and relative (in percents) experimental errors of the “experimental” Adler function are also tabulated. The error analysis is described in Appendix B. We see from the Table that the theoretical component has sizeable contribution to the total “experimental” Adler function. Its contribution increases monotonically with Q from 10% (at $Q = 0.1$ GeV) to 36% (at $Q = 1$ GeV).

To test the stability of the numerical results to the QCD corrections to the β -function, we have compared two results for the “experimental” Adler function that are obtained with the two- and four-loop exact running couplings. The pQCD component has been evaluated within CIPT⁺ at N²LO. For the parameters s_p and Λ , we have used the central values given in Table 1. In the region $Q = 0 - 1.5$ GeV, the difference between using the two or four-loop approximation to the β -function is found to be quite

Table 6 Different approximations to the “experimental” Adler function as a function of the scale. The function $D_{\text{“exp.”}}^{(k)}(Q^2)$ is constructed with the pQCD component evaluated within CIPT⁺ at N^(k-1)LO. The QCD running coupling to the four loop order is used.

Q GeV	$D_{\text{“exp.”}}^{(1)}(Q^2)$	$D_{\text{“exp.”}}^{(2)}(Q^2)$	$D_{\text{“exp.”}}^{(3)}(Q^2)$	$D_{\text{“exp.”}}^{(4)}(Q^2)$	$D_{\text{“exp.”}}^{(5)}(Q^2)$
0.1	0.06492	0.06494	0.06494	0.06494	0.06494
0.2	0.22995	0.23003	0.23004	0.23005	0.23006
0.3	0.43523	0.43540	0.43544	0.43546	0.43547
0.4	0.63164	0.63195	0.63201	0.63204	0.63207
0.5	0.79382	0.79428	0.79438	0.79443	0.79445
0.6	0.91546	0.91610	0.91623	0.91630	0.91633
0.7	1.0006	1.0015	1.0016	1.0017	1.0018
0.8	1.0571	1.0581	1.0583	1.0584	1.0585
0.9	1.0927	1.0939	1.0942	1.0943	1.0944
1.0	1.1256	1.1272	1.1276	1.1277	1.1278
1.5	1.1297	1.1320	1.1324	1.1327	1.1328

small ($\sim 0.05\%$). The approximation corresponding to the two-loop running coupling takes slightly large values.

To test the stability of numerical results to higher order perturbation theory contributions, we use various approximations to the pQCD component (see Table 6). We see from the Table that the differences between the consecutive approximations to the “experimental” Adler function slowly increase as a function of the scale. Already, the leading order approximation provides a very accurate result. At $Q = 1.5$ GeV (where the changes induced by the loop correction take maximal values) the differences between consecutive approximations (i.e. the differences between the $N^{k-1}LO$ and N^kLO approximations) take the values 0.2%, 0.04%, 0.02% and 0.01% for $k = 1, 2, 3$ and 4 respectively.

It is instructive to investigate numerically the convergence property of the non-power series for the perturbation theory component $D_{CI}(Q^2, s_p)$. The non-power series is obtained from formula (26) by using perturbation theory expansions for the function $\rho_{eff}(s)$ and $r(s)$ (see formulas (14), (18) and (25)). The non-power series read

$$D_{CI}(Q^2, s_p) = \sum_{k=0} d_k A_k(Q^2, s_p, \Lambda), \quad (48)$$

where

$$A_0(Q^2, s_p) = \frac{Q^2}{(s_p + Q^2)}, \quad (49)$$

$$A_{k \geq 1}(Q^2, s_p, \Lambda) = \frac{Q^2}{(s_0 + Q^2)} r_k(s_p) - \frac{Q^2}{\pi} \int_{s_p}^{\infty} \frac{\rho_k(Q^2)}{\sigma(\sigma + Q^2)} d\sigma, \quad (50)$$

here we have used the notations

$$\rho_k(\sigma) = \text{Im}\{a_s^k(-\sigma - i0)\}, \quad (51)$$

$$r_k(s_p) = \frac{1}{\pi} \int_{s_p}^{\infty} \frac{\rho_k(\sigma)}{\sigma} d\sigma. \quad (52)$$

Let us truncate the non-power expansion (48) at N⁴LO (i.e. for $k = 5$). Using the N⁴LO estimates for the parameters given in Table 3, we evaluate the ratios of the consecutive

Table 7 The ratios of the consecutive terms in the non-power series (48) as a function of the scale.

Q GeV	$R_1(Q^2)$	$R_2(Q^2)$	$R_3(Q^2)$	$R_4(Q^2)$	$R_5(Q^2)$
0.1	0.079	0.114	0.229	0.362	0.219
0.3	0.079	0.113	0.229	0.362	0.221
0.5	0.078	0.113	0.229	0.362	0.224
0.7	0.078	0.112	0.228	0.363	0.228
1.0	0.076	0.111	0.227	0.364	0.235
1.3	0.075	0.109	0.225	0.365	0.242
1.5	0.074	0.108	0.224	0.365	0.247
1.8	0.072	0.107	0.222	0.366	0.254
2.0	0.071	0.106	0.221	0.366	0.258

terms of the series

$$R_k(Q^2) = (d_k/d_{k-1})\mathcal{A}_k(Q^2, s_p, \Lambda)/\mathcal{A}_{k-1}(Q^2, s_p, \Lambda),$$

($k = 1 - 5$). In Table 7, we tabulate numerical values of these ratios in the region $Q = 0.1 - 2$ GeV. It is seen from the Table, that the magnitudes of the ratios are sufficiently small ($R_k(Q^2) \leq 0.366$, $k = 1, 2, \dots$ for all values of Q in the considered interval) to guarantee fast numerical convergence of the series.

Let us now compare our numerical results on the “experimental” Adler function with the previous results given in [3]. First, we repeat the calculation described in [3] with the improved data. Assuming the value $\Lambda_{\overline{\text{MS}}} = 372 \pm 76$ MeV used in [3], we solve numerically the FOPT counterpart of the equation (39). Thus we find the solution $s_p = 1.621 \pm 0.163$ GeV². The central value of this estimate is slightly large, by 0.021, than the value obtained in [3]. Using the values $s_p = 1.621$ GeV² and $\Lambda_{\overline{\text{MS}}} = 372$ MeV, we calculate the “experimental” Adler function within the (modified) FOPT at N²LO. This is compared with the new approximation which is computed in the same order within CIPT⁺. In the case of CIPT⁺, we use the values $\Lambda_{\overline{\text{MS}}} = 383$ MeV and $s_d = 1.711$ GeV² (see Table 1). To be consistent with [3], we use the two-loop exact running coupling. In Table 8, we compare numerically these approximations to the “experimental” Adler function, the functions $D_{\text{“exp.”}}^{FO}(Q^2)$ and $D_{\text{“exp.”}}^{CI}(Q^2)$. From the Table, we see that the functions are close, but $D_{\text{“exp.”}}^{FO}(Q^2) > D_{\text{“exp.”}}^{CI}(Q^2)$. The relative difference between the functions in the considered region varies in the interval 0.20% – 0.34%.

5 Conclusion

We have extracted the numerical values of the strong coupling constant α_s and the parameter s_p (the square of the boundary energy) from the non-strange vector τ data provided by ALEPH. Based on the semi-empirical representation (4) for the hadronic non-strange vector spectral function, we have developed a modified extraction procedure. This procedure enabled us to avoid direct application of the standard OPE formalism in Minkowski space. The distinguishing feature of our analysis is that we have determined the two parameters simultaneously from the data.

In Sect. 2, we have derived a violated DR for the RG improved perturbation theory correction to the Adler function (see formula (16)). Using the violated DR, we have expressed the perturbation theory part of the total “experimental” hadronic non-strange

Table 8 Comparison of the “experimental” Adler functions evaluated within the modified FOPT and CIPT⁺. The pQCD components of the functions are constructed at N²LO using the two-loop order running coupling. The function $D_{\text{“exp.”}}^{FO}(Q^2)$ has the pQCD component evaluated with the values $\Lambda_{\overline{\text{MS}}} = 372 \text{ MeV}$ and $s_d = 1.621 \text{ GeV}^2$. The pQCD component of the function $D_{\text{“exp.”}}^{CI}(Q^2)$ is evaluated using the values $\Lambda_{\overline{\text{MS}}} = 383 \text{ MeV}$ and $s_d = 1.711 \text{ GeV}^2$. The relative difference between these functions is also tabulated.

$Q \text{ GeV}$	$D_{\text{“exp.”}}^{FO}(Q^2)$	$D_{\text{“exp.”}}^{CI}(Q^2)$	rel.diff.
0.1	0.0651	0.0649	0.31%
0.2	0.2305	0.2301	0.20%
0.3	0.4364	0.4355	0.21%
0.4	0.6336	0.6321	0.24%
0.5	0.7967	0.7945	0.28%
0.6	0.9191	0.9164	0.29%
0.7	1.0050	1.0018	0.32%
0.8	1.0621	1.0586	0.33%
0.9	1.0982	1.0945	0.34%
1.0	1.1197	1.1160	0.33%
1.1	1.1316	1.1280	0.32%
1.2	1.1371	1.1337	0.30%
1.3	1.1386	1.1355	0.27%
1.4	1.1377	1.1350	0.24%
1.5	1.1354	1.1330	0.21%

vector spectral function in terms of the effective spectral density, $\rho_{eff}(\sigma)$, the basis object of the perturbation theory calculation (see formula (23)). We have then obtained a convenient expression for the pQCD part of the “experimental” Adler function in terms of the effective spectral function (see formula (26)). Making further use of the consistency condition from the OPE for the “experimental” Adler function, we have derived Eq. (34). This equation relates the parameters s_p and Λ to the values of the hadronic spectral function on the range $0 < s < s_p$. Next we used the *ansatz* (4) for the spectral function to calculate the τ decay rate $R_{\tau,V}$. In this way, we have derived Eq. (37) which relates the parameters to the integral of the hadronic spectral function (multiplied by known function) over the range $s_p < s < m_\tau^2$.

In Sect. 3, we have solved, numerically, the obtained system of equations for the parameters s_p and $\Lambda \equiv \Lambda_{\overline{\text{MS}}}$. To examine the convergence of the numerical results for the extracted parameters, we have used perturbation theory approximations to the Adler function up to the N⁴LO. As a criterion of the quality of the approximations, the indicative estimates of the theoretical errors introduced in [22] are used. With this criterion, we have demonstrated that the new framework (CIPT⁺), compared to the standard one (CIPT), provides better numerical convergence for the value of the coupling constant $\alpha_s(m_\tau^2)$. The central values of the coupling constant extracted within CIPT⁺ at N²LO, N³LO and N⁴LO practically coincide (see Eq. (45) and Table 4). It is remarkable that the central values of the coupling constant extracted within CIPT⁺ at different orders of perturbation theory become systematically smaller as compared to the standard values obtained at the same orders within CIPT (cf. formulas (45) and (46)). The changes in the central values are not within the quoted experimental errors. However, we remark that the new procedure as compared to the standard one has a shortcoming. It leads to more large experimental error (by the factor ~ 2) on the coupling constant. Nevertheless, the central values of $\alpha_s(m_\tau^2)$ in formulas (45) and (46) differ from each other in about 1.7 standard deviation.

We have also confirmed that the extracted numerical value for the parameter s_p is remarkable stable against perturbation theory corrections. The associated indicative theoretical error systematically decreases with the order of the approximation. Thus to the $N^3\text{LO}$ and $N^4\text{LO}$ orders the errors take the values 0.03% and 0.01% respectively. Our result for the central value of this parameter is higher in about 7% compared to the value obtained previously in [3].

Our prediction for the strong coupling constant is in good agreement with the recent high precision determination of $\alpha_s(m_\tau^2)$ presented in [16]. Their estimate within CIPT (extracted from the non-strange vector τ data provided by ALEPH) is

$$\alpha_s(m_\tau^2) = 0.321 \pm 0.007_{exp.} \pm 0.012_{th.} \quad (53)$$

In this work, particular sum rules derived within CIPT and FOPT have been employed to suppress the contributions associated with poorly known higher dimension condensates. These contributions are known to be large in the vector and axial vector separate channels. Remarkably, the central values of the coupling constant in formulas (53) and (45) coincide. Our approach based on a different technique confirms that there is a theoretical systematic uncertainty not included in the error assessments obtained in previous studies by ignoring the higher order OPE contributions, the conclusion achieved in work [16]. In this connection, our study suggests that the truncated OPE series cannot approximate sufficiently accurately the integrals of the spectral function over the low energy region $0 < s < s_p \sim 1.7 \text{ GeV}^2$.

In Sect. 4, we have recalculated the “experimental” Adler function within the CIPT^+ prescription using the new estimates for the parameters s_p and Λ . In addition, we have determined the errors on this function coming from the uncertainties of the parameters and spectral function. Numerical results for the Adler function obtained within CIPT^+ have been found to be remarkable stable in perturbation theory. To check the numerical stability we have used the pQCD components for the Adler function up to (and including) $N^4\text{LO}$ (see Tables 6 and 7).

In Appendix A, we have given practical formulas for numerical calculation of the $\overline{\text{MS}}$ running coupling at higher orders. The Lambert-W solutions to the RG equation have been reviewed. A very accurate analytic approximation to the effective spectral density $\rho_{eff}(\sigma)$ at higher orders is derived. In Appendix B, we have derived formulas within CIPT^+ for calculating the experimental uncertainties on the extracted values of the parameters. A formula for calculating the errors on the “experimental” Adler function is also derived. In Appendix C, we have analyzed the ALEPH (non-strange vector) τ -data within the standard CIPT prescription: We have performed some necessary calculations needed for comparing the CIPT and CIPT^+ prescriptions (see Sect. 3).

The procedure suggested here can obviously be extended to analyze the non-strange τ -data from the axial-vector (A) and vector plus axial-vector (V+A) channels. This may be done by extending the *ansatz* (4) to the axial-vector hadronic spectral function too. To check the reliability of the new extraction procedure, it is desirable to compare the V, A, and V+A determinations of the coupling constant. To estimate total theoretical errors on the extracted values of the parameters Λ and s_p , it is mandatory to define an analogical procedure within the FOPT prescription too. It should be remarked that a shortcoming of the *ansatz* (4) is that it completely ignores the non-perturbative contributions to the spectral function coming from the region $s > s_p$. The importance of these contributions for accurate determination of the coupling constant has been demonstrated in recent study [10]. We hope to report on these aspects in future publications.

Acknowledgements I am very grateful for the support of my colleagues at Department of Theoretical Physics at Andrea Razmadze Mathematical Institute. The present work has been partially supported by the Georgian National Science Foundation under grants No GNSF/ST08/4-405 and No GNSF/ST08/4-400.

A A Series Solution to the Renormalization Group Equation

In our notation the RG equation for the running coupling reads

$$\frac{d}{d \ln Q^2} a_s = \beta(a_s) = -a_s^2 \sum_{n=0} \beta_n a_s^n, \quad (54)$$

where $a_s \equiv a_s(Q^2) = \frac{\alpha_s(Q^2)}{\pi}$ with $\alpha_s(Q^2)$ being the running coupling. In the $\overline{\text{MS}}$ scheme, the β -function coefficients are known to four loops [57]. For three active quark flavours the first four coefficients take the values

$$\beta_0 = 2.25, \quad \beta_1 = 4, \quad \beta_2 = 10.05990, \quad \beta_3 = 47.22804.$$

In general, the RG equation (54), to an arbitrary order in perturbation theory, can not be solved explicitly for the coupling. Usually, the equation is solved in the asymptotical regime $\frac{Q^2}{\Lambda^2} \gg 1$. For our purposes the asymptotic solution is not suitable, since we need an accurate solution at relatively low energies. One may, of course, solve the RG equation numerically. However, it is more convenient to derive some accurate analytic approximation to the coupling. Fortunately, it is possible to solve the RG equation explicitly for the coupling at the two loop order [25, 26]. The explicit expression for the $\overline{\text{MS}}$ scheme running coupling at the two loop order reads

$$a_s^{(2)}(Q^2) = -\frac{\beta_0}{\beta_1} \frac{1}{1 + W_{-1}(\zeta)} : \quad \zeta = -\frac{1}{e b_1} \left(\frac{Q^2}{\Lambda^2} \right)^{-1/b_1}, \quad (55)$$

where β_0 and β_1 are the first two β -function coefficients

$$\beta_0 = \frac{1}{4} \left(11 - \frac{2}{3} n_f \right), \quad \beta_1 = \frac{1}{16} \left(102 - \frac{38}{3} n_f \right),$$

$b_1 = \beta_1/\beta_0^2$, $\Lambda \equiv \Lambda_{\overline{\text{MS}}}$ and W_{-1} denotes the branch of the Lambert W function [58].

The coupling to higher orders may be expanded in powers of the two loop order coupling [50, 51]

$$a_s^{(k>2)}(Q^2) = \sum_{n=1}^{\infty} c_n^{(k)} a_s^{(2)n}(Q^2), \quad (56)$$

The first two coefficients in this series are universal: $c_1^{(k)} = 1$ and $c_2^{(k)} = 0$ (the condition $c_2^{(k)} = 0$ follows from the conventional definition of the Λ parameter). Other coefficients are determined in terms of the β -function coefficients. The four-loop expressions for the first several coefficients are given by

$$c_3^{(4)} = \frac{\beta_2}{\beta_0}, \quad c_4^{(4)} = \frac{\beta_3}{2\beta_0}, \quad c_5^{(4)} = \frac{5}{3} \left(\frac{\beta_2}{\beta_0} \right)^2 - \frac{\beta_1\beta_3}{6\beta_0^2}, \dots$$

It was proved in [28] that the series has a finite radius of convergence, and the radius is sufficiently large for all n_f values of practical interest. Partial sums of the series (56) provide very accurate approximations to the higher order coupling in the wide range of Q^2 . In particular, these approximations may be safely used at low energies. Thus, for $Q = 1$ GeV and $\Lambda = 0.347$ GeV, the partial sum with the first twelve terms reproduce the exact four loop coupling with the precision better than 0.02%. Using the exact solution (55), the analytical structure of the two loop coupling in the complex Q^2 -plane has been determined [25, 26]. It was found that the coupling is an analytic function in the whole complex plane except the cuts running along the real Q^2 axis. Besides the physical cut $\{Q^2 : -\infty < Q^2 < 0\}$ corresponding

Table 9 Numerical values of the first twelve coefficients in the expansion (56) for the four loop running coupling at $n_f = 3$ quark flavours.

n	c_n		n	c_n
1	1		7	392.1241
2	0		8	2413.463
3	3863/864		9	8248.857
4	10.49512		10	31348.18
5	27.09804		11	147697.8
6	190.2642		12	507565.0

to the logarithmic singularity at $Q^2 = 0$, there is also the “Landau” cut $\{Q^2 : 0 < Q^2 < Q_L^2\}$ corresponding to the Landau singularity on the positive Q^2 -axis. The Landau singularity is a second order algebraic branch point located at $Q_L^2 = b_1^{-b_1} \Lambda^2$ ($b_1^{-b_1} \approx 1.205$ for $n_f = 3$). The relevant branch of the Lambert function on the complex Q^2 plane is determined by the analytical continuation. For the physical vales of n_f ($0 < n_f \leq 6$) the relevant branch is W_{-1} on the upper-half plane, whereas the branch is W_1 on the lower-half plane. A limiting value of the coupling from above the physical cut ($Q^2 = -\sigma + i0$, $\sigma > 0$) is then determined by [27]

$$a_s^{(2)}(-\sigma + i0) = -\frac{\beta_0}{\beta_1} \frac{1}{1 + W_{-1}(\zeta_+)} \quad \text{with} \quad \zeta_+ = \frac{1}{eb_1} \left(\frac{\sigma}{\Lambda^2} \right)^{-1/b_1} \exp \left\{ -i\pi \left(\frac{1}{b_1} - 1 \right) \right\}, \quad (57)$$

similarly, one may write

$$a_s^{(2)}(-\sigma - i0) = -\frac{\beta_0}{\beta_1} \frac{1}{1 + W_1(\zeta_-)} \quad \text{with} \quad \zeta_- = \frac{1}{eb_1} \left(\frac{\sigma}{\Lambda^2} \right)^{-1/b_1} \exp \left\{ i\pi \left(\frac{1}{b_1} - 1 \right) \right\}. \quad (58)$$

Note that the limiting values $a_s^{(2)}(-\sigma \pm i0)$ satisfy the Schwarz ‘principle of reflection’,

$a_s^{(2)}(-\sigma - i0) = \overline{a_s^{(2)}(-\sigma + i0)}$, provided that W has *near conjugate* symmetry [58]:
 $W_k(\bar{z}) = W_{-k}(z)$.

With formula (56) for the four-loop running coupling, we may construct an analytic approximation to the Adler function in perturbation theory. In this approximation, the Adler function is an analytic function in the cut complex Q^2 plane. It has the branch points at $Q^2 = 0$ and $Q^2 = Q_L^2 = b_1^{-b_1} \Lambda^2 > 0$. The effective spectral density (18) associated with the Adler function is then readily calculated, leading to the analytic expression

$$\rho_{eff.}(\sigma) = \text{Im} \left\{ \sum_{n=1}^N d_n \left(\sum_{m=1}^N c_m^{(4)} a_s^{(2)m}(-\sigma - i0) \right)^n \right\}, \quad (59)$$

where $N \geq 3$ and $a_s^{(2)}(-\sigma - i0)$ is determined in terms of the W function as given in formula (58). Formula (59) considerably simplifies numerical calculations of integrals of the effective spectral function (computer algebra system Maple has an arbitrary precision implementation of all branches of the Lambert function). In the most of the calculations, we have used the truncated series (56) for the four loop running coupling preserving the first twelve terms in the series. Numerical values of the first twelve coefficients of the series, for $n_f = 3$ quark flavours, are tabulated in Table 9.

B The Error Analysis

In this appendix we will evaluate the experimental errors on the extracted values of the parameters. We will also determine the errors on the “experimental” Adler function. The main quantity employed in our analysis is the vector (non-strange) spectral function $v_1(s)$. It is related with the vector invariant mass squared distribution (the function $sfm2(s)$ in the notations of [12])

$$v_1(s) = \kappa(s) sfm2(s), \quad (60)$$

Table 10 A few measured values of $sfm2(s)$ and $v_1(s)$. The standard errors for these quantities are indicated.

$s \text{ GeV}^2$	$sfm2(s)$	$\sigma_{sfm2}(s)$	$v_1(s)$	$\sigma_{v1}(s)$
0.0875	0.004923	0.001251	0.006027	0.001531
0.1125	0.022630	0.003092	0.027745	0.003791
0.1375	0.037048	0.004520	0.045504	0.005551
0.1625	0.056542	0.005747	0.069597	0.007074
0.1875	0.073407	0.005875	0.090583	0.007250
0.2125	0.095429	0.006541	0.118095	0.008095
0.2375	0.122440	0.007574	0.152005	0.009403

the kinematical factor $\kappa(s)$ is

$$\kappa(s) = \mathcal{N} \frac{m_\tau^2}{(6|V_{ud}|^2 S_{EW})} \left(\frac{B_V}{B_e} \right) \frac{1}{(1 - s/m_\tau^2)^2 (1 + 2s/m_\tau^2)}, \quad (61)$$

where $|V_{ud}| = 0.9746 \pm 0.0006$ denotes the flavor mixing matrix elements, the factor $S_{EW} = 1.0198 \pm 0.0006$ is an electro-weak correction term, $m_\tau = 1777.03^{+0.3}_{-0.26} \text{ MeV}$, $B_V = (31.82 \pm 0.22)\%$ and $B_e = (17.810 \pm 0.039)\%$ are the vector and leptonic branching fractions respectively (in this paper, we assume these estimates following [11]), \mathcal{N} is the normalizing constant

$$\mathcal{N} = \left\{ \int_0^{m_\tau^2} sfm2(s) ds \right\}^{-1} \approx \frac{1}{0.794748}.$$

The quantity $sfm2(s)$ is measured at 140 equidistant values of the energy squared variable starting from $s_1 = 0.0125 \text{ GeV}^2$ with the bin size $\Delta_{bin} = 0.025 \text{ GeV}^2$. Note that the factor $\kappa(s)$ is determined within an accuracy of less than 1% for all values of s in the range $s = 0 - m_\tau^2$, while the errors in determination of $sfm2(s)$ are considerably large. Hence, it is safe to ignore the uncertainties coming from the factor $\kappa(s)$. We may then write

$$\sigma_{v1}[k] = |\kappa(s_k)| \sigma_{sfm2}[k], \quad k = 1, \dots, 140 \quad (62)$$

where $\sigma_{v1}[k]$ and $\sigma_{sfm2}[k]$ stand for the standard deviations of $v_1(s_k)$ and $sfm2(s_k)$ respectively, and $s_k = s_1 + (k-1)\Delta_{bin}$ ($k=1, 2, \dots$). By definition

$$\sigma_{v1}^2[k] = \mathbf{E}[(v_1(s_k) - \overline{v_1(s_k)})^2], \quad (63)$$

etc ¹². Similarly, the covariance matrices of the errors associated with the quantities $v_1(s)$ and $sfm2(s_k)$ are related by the formula

$$\mathbb{C}_{ik} = \kappa(s_i) \kappa(s_k) \tilde{\mathbb{C}}_{ik}, \quad (64)$$

where $\mathbb{C}_{ik} = \text{cov}(v_1(s_i), v_1(s_k))$ and $\tilde{\mathbb{C}}_{ik} = \text{cov}(sfm2(s_i), sfm2(s_k))$. So that respective correlation coefficients coincide

$$\mathbb{R}_{kl} = \frac{\mathbb{C}_{kl}}{\sigma_{v1}[k] \sigma_{v1}[l]} = \frac{\tilde{\mathbb{C}}_{kl}}{\sigma_{sfm2}[k] \sigma_{sfm2}[l]}. \quad (65)$$

In Table 10, we present a few measured values of $sfm2(s)$ and $v_1(s)$ together with the associated uncertainties. Our goal is to estimate the uncertainties on the extracted values of the parameters induced from the experimental uncertainties of the spectral function. We start from the system of (39)-(40), which we rewrite in the form

$$\Phi_1(x, y) = \mathcal{E}_1(x, \{v_1\}) \quad (66)$$

$$\Phi_2(x, y) = \mathcal{E}_2(x, \{v_1\}) \quad (67)$$

¹² The symbol $\mathbf{E}[x]$ refers to the average of x .

where we have introduced the notations $x = s_p$, $y = \Lambda^2$ and

$$\begin{aligned}\mathcal{E}_1(x, \{v_1\}) &= \int_0^x v_1(t) dt \\ \mathcal{E}_2(x, \{v_1\}) &= \int_x^{m_\tau^2} w_\tau(t) v_1(t) dt,\end{aligned}$$

to avoid a cumbersome notation the superscript “exp.” in function $v_1^{\text{exp.}}(s)$ has been omitted. The solution to the system (66)-(67) should be considered as a functional of $v_1(s)$. Let a solution for the parameters, for a given function $v_1(s)$, is

$$x = \psi_1(\{v_1\}) \quad (68)$$

$$y = \psi_2(\{v_1\}). \quad (69)$$

we may write $v_1(s) = \bar{v}_1(s) + \delta v_1(s)$, where $\bar{v}_1(s)$ is the central (average) value and $\delta v_1(s)$ is the deviation. The central values of the parameters should be determined by solving the system (66)-(67) for $v_1(x) = \bar{v}_1(x)$ (see, for example, the book [56]) i.e.

$$\bar{x} = \psi_1(\{\bar{v}_1\}) \quad (70)$$

$$\bar{y} = \psi_2(\{\bar{v}_1\}). \quad (71)$$

Let us expand the functionals $\mathcal{E}_{1,2}(x, \{v_1\})$ in powers of a small variation $\delta v_1(s)$, preserving the terms linear in δx and $\delta v_1(s)$

$$\mathcal{E}_1(x, \{v_1\}) = \Phi_1(\bar{x}, \bar{y}) + \delta x \bar{v}_1(\bar{x}) + \int_0^{\bar{x}} \delta v_1(t) dt + \dots \quad (72)$$

$$\mathcal{E}_2(x, \{v_1\}) = \Phi_2(\bar{x}, \bar{y}) - w_\tau(\bar{x}) \bar{v}_1(\bar{x}) \delta x + \int_{\bar{x}}^{m_\tau^2} w_\tau(t) \delta v_1(t) dt + \dots, \quad (73)$$

here use has been made of the equations $\mathcal{E}_{1,2}(\bar{x}, \{\bar{v}_1\}) = \Phi_{1,2}(\bar{x}, \bar{y})$. Insert these expansions into Eqs.(66)-(67) and expand the left hand sides of the equations in powers of δx and δy

$$\Phi_{1,2}(x, y) = \Phi_{1,2}(\bar{x}, \bar{y}) + \frac{\partial \Phi_{1,2}(\bar{x}, \bar{y})}{\partial \bar{x}} \delta x + \frac{\partial \Phi_{1,2}(\bar{x}, \bar{y})}{\partial \bar{y}} \delta y + \dots$$

Retaining terms linear in δx , δy and δv_1 , we are led to the following linear algebraic system of equations for the variations δx and δy

$$\begin{aligned}A_1 \delta x + B_1 \delta y &= G_1 \\ A_2 \delta x + B_2 \delta y &= G_2,\end{aligned} \quad (74)$$

where

$$\begin{aligned}A_1 &= \frac{\partial \Phi_1(\bar{x}, \bar{y})}{\partial \bar{x}} - \bar{v}_1(\bar{x}), \quad B_1 = \frac{\partial \Phi_1(\bar{x}, \bar{y})}{\partial \bar{y}}, \quad G_1 = \int_0^{\bar{x}} \delta v_1(t) dt, \\ A_2 &= \frac{\partial \Phi_2(\bar{x}, \bar{y})}{\partial \bar{x}} + w_\tau(\bar{x}) \bar{v}_1(\bar{x}), \quad B_2 = \frac{\partial \Phi_2(\bar{x}, \bar{y})}{\partial \bar{y}}, \quad G_2 = \int_{\bar{x}}^{m_\tau^2} w_\tau(t) \delta v_1(t) dt.\end{aligned}$$

Using the explicit formulas (41) and (42), after some algebra, we obtain

$$\begin{aligned}\frac{\partial \Phi_1(x, y)}{\partial x} &= \frac{(1 + r(x))}{2} \\ \frac{\partial \Phi_1(x, y)}{\partial y} &= \frac{1}{2\pi} \int_{-\infty}^{\ln(x/y)} \tilde{\rho}_{eff}(t) e^t dt + \frac{c_L}{2} \\ \frac{\partial \Phi_2(x, y)}{\partial x} &= -\frac{(1 + r(x))}{4m_\tau^2} P\left(\frac{x}{m_\tau^2}\right) \\ \frac{\partial \Phi_2(x, y)}{\partial y} &= \frac{1}{4\pi m_\tau^2} \int_{\ln(x/y)}^{\ln(m_\tau^2/y)} \tilde{\rho}_{eff}(t) e^t P\left(\frac{ye^t}{m_\tau^2}\right),\end{aligned}$$

where $\tilde{\rho}_{eff}(t) \equiv \rho_{eff}(\sigma)$ with $\sigma = \Lambda^2 \exp(t)$, $P(z) = 2(z-1)^2(2z+1)$, and $r(s)$ is defined in (25). After solving the system (74), we take the averages of the deviations squared (the variances)

$$\begin{aligned} \overline{(\delta x)^2} &= (B_2^2 \overline{G_1^2} + B_1^2 \overline{G_2^2} - 2B_1 B_2 \overline{G_1 G_2}) / \mathcal{D}^2 \\ \overline{(\delta y)^2} &= (A_1^2 \overline{G_2^2} + A_2^2 \overline{G_1^2} - 2A_1 A_2 \overline{G_1 G_2}) / \mathcal{D}^2, \end{aligned} \quad (75)$$

where $\mathcal{D} = A_1 B_2 - A_2 B_1$, and the overlined symbols refer to the averages: $\overline{(\delta x)^2} = E[(x - \bar{x})^2]$ etc. To calculate the averages $\overline{G_1^2}$, $\overline{G_2^2}$ and $\overline{G_1 G_2}$ we replace the integrals $G_{1,2}$ by sums over the equidistant mesh, using the trapezoidal rule,

$$G_1 \approx \Delta \sum_{k=1}^{n_p} g_k \delta v_1(t_k), \quad G_2 \approx \Delta \sum_{k=n_p}^{n_\tau} \eta_k \delta v_1(t_k) \quad (76)$$

where $n_p = 1 + [(\bar{s}_p - s_1)/\Delta]_{\text{round}}$, $n_\tau = 1 + [(m_\tau^2 - s_1)/\Delta]_{\text{round}}$ ¹³, Δ denotes the width of the mesh which is identified with the bin size in the data. The mesh points in the sums are determined by $t_k = t_1 + (k-1)\Delta$, $k = 1, 2, \dots$, with $t_1 = 0.0125$ and $\Delta = 0.025$. The numerical coefficients g_k take the values $g_k = 1$ for $1 < k < n_p$ and $g_1 = g_{n_p} = 0.5$. The factors η_k are determined by

$$\begin{cases} \eta_k = w_\tau(t_k) & \text{if } n_p < k < n_\tau. \\ \eta_k = 0.5 w_\tau(t_k) & \text{if } k = n_p \text{ or } k = n_\tau. \end{cases}$$

Using formula (76) and taking into account the definitions (63) and (64), we calculate the required averages

$$\overline{G_1^2} = (\Delta)^2 \left(\sum_{k=1}^{n_p} g_k^2 \sigma_{v_1}^2[k] + 2 \sum_{k=1}^{n_p-1} \sum_{l>k}^{n_p} g_k g_l \mathbb{C}_{kl} \right), \quad (77)$$

$$\overline{G_2^2} = (\Delta)^2 \left(\sum_{k=n_p}^{n_\tau} \eta_k^2 \sigma_{v_1}^2[k] + 2 \sum_{k=n_p}^{n_\tau-1} \sum_{l=k+1}^{n_\tau} \eta_k \eta_l \mathbb{C}_{kl} \right), \quad (78)$$

$$\overline{G_1 G_2} = (\Delta)^2 \sum_{k=1}^{n_p} \sum_{l=n_p}^{n_\tau} g_k \eta_l \mathbb{C}_{kl}. \quad (79)$$

We are now in a position to determine the uncertainties on the values of the “experimental” Adler function. They are induced from the errors of the experimental spectral function and from the errors on the parameters Λ and s_p . Let us represent again the “experimental” Adler function as a sum of the two terms showing explicitly the dependence of the terms on the parameters and on the spectral function

$$D_{\text{“exp.”}}(Q^2, \Lambda^2, s_p : v_1) = D_{\text{exp.}}(Q^2, s_p : v_1) + D_{pQCD}(Q^2, \Lambda^2, s_p), \quad (80)$$

the experimental and pQCD parts of the function are determined as

$$D_{\text{exp.}}(Q^2, s_p : v_1) = \int_0^{s_p} \mathcal{K}(Q^2, t) v_1(t) dt \quad (81)$$

$$D_{pQCD}(Q^2, \Lambda^2, s_p) = \int_{s_p}^\infty \mathcal{K}(Q^2, t) v_1^{CI}(t) dt, \quad (82)$$

where $\mathcal{K}(Q^2, t) = 2Q^2/(t + Q^2)^2$, $v_1(s)$ denotes the spectral function measured on the experiment ($v_1(s) \equiv v_1^{\text{exp.}}(s)$) and $v_1^{CI}(s)$ is the approximation to the spectral function evaluated within CIPT. Consider small deviations of the spectral function and the parameters from their mean values

$$v_1(t) = \bar{v}_1(t) + \delta v_1(t), \quad s_p = \bar{s}_p + \delta s_p, \quad \Lambda^2 = \bar{\Lambda}^2 + \delta \Lambda^2, \quad (83)$$

¹³ here the subscript “round” refers to the integer nearest to the number inside the square bracket.

the change of the “experimental” Adler function under these variations is

$$\delta D^{\text{“exp.”}} = \delta D_{\text{exp.}} + \delta D_{pQCD}, \quad (84)$$

here we have used abbreviations $D_{\text{exp.}} \equiv D_{\text{exp.}}(Q^2, s_p : v_1)$ etc. The right hand side of (84) can be evaluated using formulas (81) and (82). Preserving terms linear in the variations δv_1 , δs_p and $\delta \Lambda^2$, we find

$$\delta D^{\text{“exp.”}} = \delta v_1 D_{\text{exp.}} + E_{\bar{s}_p} \delta s_p + E_{\bar{\Lambda}^2} \delta \Lambda^2 \quad (85)$$

where

$$\delta v_1 D_{\text{exp.}} = \int_0^{\bar{s}_p} \mathcal{K}(Q^2, t) \delta v_1(t) dt, \quad (86)$$

$$E_{\bar{s}_p} = \mathcal{K}(Q^2, \bar{s}_p) \bar{v}_1(\bar{s}_p) + \frac{\partial D_{pQCD}(Q^2, \bar{\Lambda}^2, \bar{s}_p)}{\partial \bar{s}_p}, \quad (87)$$

$$E_{\bar{\Lambda}^2} = \frac{\partial D_{pQCD}(Q^2, \bar{\Lambda}^2, \bar{s}_p)}{\partial \bar{\Lambda}^2}. \quad (88)$$

Using the trapezoidal rule, we approximate the integral on the right side of Eq. (86)

$$\delta v_1 D_{\text{exp.}} \approx G_3 = \sum_{k=1}^{n_p} g_k \mathcal{K}(Q^2, t_k) \delta v_1(t_k), \quad (89)$$

where the quantities n_p , g_k and t_k are defined below the formula (76). To calculate the partial derivatives on the right hand sides of (87) and (88), we use the explicit formula (26) for the pQCD part of the Adler function. We then obtain

$$\begin{aligned} \frac{\partial D_{pQCD}(Q^2, \Lambda^2, s_p)}{\partial s_p} &= -\frac{Q^2}{(Q^2 + s_p)^2} (1 + r(s_p)) \\ \frac{\partial D_{pQCD}(Q^2, \Lambda^2, s_p)}{\partial \Lambda^2} &= \frac{1}{\pi Q^2} \int_{\ln(s_p/\Lambda^2)}^{\infty} \frac{e^t \tilde{\rho}_{eff}(t)}{\left(1 + \frac{\Lambda^2}{Q^2} e^t\right)^2} dt, \end{aligned}$$

to derive the last formula we have used the relation

$$\frac{\partial r(s_p)}{\partial \Lambda^2} = \frac{1}{\pi \Lambda^2} \rho_{eff}(s_p),$$

which can be easily derived from the definition (25). The mean squared deviation of the “experimental” Adler function is then determined as a sum of the six averages

$$\begin{aligned} \overline{(\delta D^{\text{“exp.”}})^2} &= \overline{(\delta v_1 D_{\text{exp.}})^2} + E_{\bar{s}_p}^2 \overline{(\delta s_p)^2} + E_{\bar{\Lambda}^2}^2 \overline{(\delta \Lambda^2)^2} \\ &\quad + 2E_{\bar{s}_p} E_{\bar{\Lambda}^2} \overline{\delta s_p \delta \Lambda^2} + 2E_{\bar{s}_p} \overline{(\delta v_1 D_{\text{exp.}}) \delta s_p} + 2E_{\bar{\Lambda}^2} \overline{(\delta v_1 D_{\text{exp.}}) \delta \Lambda^2}. \end{aligned} \quad (90)$$

With the aid of formula (89), the first term on the right of Eq. (90) can easily be expressed in terms of the errors σ_{v_1} and the covariance matrix \mathbb{C}_{kl}

$$\overline{(\delta v_1 D_{\text{exp.}})^2} = \Delta^2 \left\{ \sum_{k=1}^{n_p} g_k^2 \mathcal{K}^2(Q^2, t_k) \sigma_{v_1}^2[k] + 2 \sum_{k=1}^{n_p-1} \sum_{l=k+1}^{n_p} g_k g_l \mathcal{K}(Q^2, t_k) \mathcal{K}(Q^2, t_l) \mathbb{C}_{kl} \right\}. \quad (91)$$

The second and third terms on the right of (90) are determined in terms of the errors σ_{s_p} and σ_{Λ^2} which we have already evaluated above (see (75)). In order to evaluate last three terms on the right of (90), we use explicit expressions for the deviations δs_p and $\delta \Lambda^2$

$$\begin{aligned} \delta s_p &= \mathcal{D}^{-1} (B_2 G_1 - B_1 G_2) \\ \delta \Lambda^2 &= \mathcal{D}^{-1} (A_1 G_2 - A_2 G_1), \end{aligned} \quad (92)$$

the solution to the system (74). This enable us to write

$$\overline{\delta s_p \delta \Lambda^2} = \mathcal{D}^{-2} \{ (B_2 A_1 + B_1 A_2) \overline{G_1 G_2} - B_2 A_2 \overline{G_1^2} - B_1 A_1 \overline{G_2^2} \}, \quad (93)$$

the averages on the right hand side of (93) have been evaluated above (see Eqs. (77), (78) and (79)). It remains to calculate the last two averages on the right hand side of (90). Using formulas (92) we find

$$\overline{(\delta_{v_1} D_{exp.}) \delta s_p} = \overline{G_3 \delta s_p} = \mathcal{D}^{-1} (B_2 \overline{G_1 G_3} - B_1 \overline{G_2 G_3}) \quad (94)$$

$$\overline{(\delta_{v_1} D_{exp.}) \delta \Lambda^2} = \overline{G_3 \delta \Lambda^2} = \mathcal{D}^{-1} (A_1 \overline{G_2 G_3} - A_2 \overline{G_1 G_3}), \quad (95)$$

employing now the trapezoidal sums (76) and (89), we determine the averages $\overline{G_1 G_3}$ and $\overline{G_2 G_3}$

$$\begin{aligned} \overline{G_1 G_3} &= \Delta^2 \sum_{k=1}^{n_p} g_k \sigma_{v_1}[k] \sum_{l=1}^{n_p} g_l \mathcal{K}(Q^2, t_l) \mathbb{R}_{k,l} \sigma_{v_1}[l], \\ \overline{G_2 G_3} &= \Delta^2 \sum_{k=n_p}^{n_\tau} \eta_k \sigma_{v_1}[k] \sum_{l=1}^{n_p} g_l \mathcal{K}(Q^2, t_l) \mathbb{R}_{k,l} \sigma_{v_1}[l], \end{aligned}$$

where $\mathbb{R}_{k,l}$ denotes the correlation coefficients given in formula (65).

C Standard CIPT Consideration

It is instructive to compare the modified procedure for extracting the coupling constant with the standard procedure formulated within conventional CIPT in the $\overline{\text{MS}}$ scheme. The conventional CIPT approach may be recovered from formula (4) by taking the limit $s_p \rightarrow 0$ and introducing the non-perturbative contributions via the OPE. Possible duality violations are then ignored. The τ decay rate to the non-strange hadrons in the vector channel is approximated as [6]

$$R_{\tau,V} = \frac{3}{2} |V_{ud}|^2 S_{EW} (1 + \delta_{QCD} + \delta_{EW}) \quad (96)$$

where δ_{QCD} represents the QCD corrections, $|V_{ud}| = 0.9746 \pm 0.0006$ is the flavor mixing matrix element, $S_{EW} = 1.0198$ is an electro-weak correction term and $\delta_{EW} \approx 0.001$ is an additive electroweak correction (for this values see [11]). The QCD contribution is the sum

$$\delta_{QCD} = \delta^{(0)} + \delta^{(2)} + \delta_{NP}, \quad (97)$$

where $\delta^{(0)}$ is the purely perturbative contribution, $\delta^{(2)}$ is the dimension $D = 2$ effects from light quark masses, and δ_{NP} is the total non-perturbative contribution: $\delta_{NP} = \delta^{(4)} + \delta^{(6)} + \delta^{(8)}$ ($\delta^{(D)}$ are the OPE terms in powers of m_τ^{-D}). We will use the estimates $\delta^{(2)} = (-3.3 \pm 3) \times 10^{-4}$ and $\delta_{NP} = 0.0199 \pm 0.0027$, the ALEPH results obtained within the CIPT approach [11]. The experimental result for $\delta^{(0)}$ can be determined from the experimental spectral function via the relation

$$1 + \delta_{exp.}^{(0)} + \delta^{(2)} + \delta_{NP} + \delta_{EW} = 4 A_{\tau,v}^{exp.}, \quad (98)$$

where

$$A_{\tau,v}^{exp.} = \int_0^{m_\tau^2} w_\tau(s) v_1^{exp.}(s) ds, \quad (99)$$

and explicit expression of the function $w_\tau(s)$ is given in (36). The relation (98) follows from formulas (36) and (96). Let us now determine the experimental error on $A_{\tau,v}^{exp.}$ induced from the experimental errors on $v_1^{exp.}(s)$. Using the trapezoidal rule, we replace the integral on the right side of Eq. (99) by the sum

$$A_{\tau,v}^{exp.} = \Delta \sum_{k=1}^{N_\tau} g_k w_\tau(s_k) v_1(s_k) \quad (100)$$

Table 11 Numerical values for the QCD scale parameter and strong coupling constant in the $\overline{\text{MS}}$ scheme for three active flavours extracted from the non-strange vector τ lepton data within the conventional CIPT approach. The results obtained in consecutive orders of perturbation theory are given. The error bars refer to the experimental uncertainty only.

Orders in perturbation theory	Λ GeV	$\alpha_s(m_\tau^2)$
LO	0.604 ± 0.023	0.485 ± 0.019
NLO	0.469 ± 0.018	0.390 ± 0.011
N ² LO	0.430 ± 0.016	0.367 ± 0.009
N ³ LO	0.407 ± 0.015	0.354 ± 0.008
N ⁴ LO	0.395 ± 0.015	0.347 ± 0.008

where $N_\tau = 1 + [(m_\tau^2 - s_1)/\Delta]_{\text{round}}$, $s_k = s_1 + (k-1)\Delta$ with $s_1 = 0.0125$ and $\Delta = 0.025$, and g_k are the numeric coefficients associated with the trapezoidal rule. From formula (100) one easily evaluates the standard error on $A_{\tau,v}^{exp.}$

$$\sigma(A_{\tau,v}^{exp.}) = \Delta \left[\sum_{k=1}^{N_\tau} \sum_{n=1}^{N_\tau} g_k g_n w_\tau(s_k) w_\tau(s_n) \mathbb{C}_{k,n} \right]^{\frac{1}{2}} \quad (101)$$

where \mathbb{C} denotes the covariance matrix $\mathbb{C}_{i,k} = \mathbf{E}[(v_1(s_i) - \overline{v_1(s_i)})(v_1(s_k) - \overline{v_1(s_k)})]$ which is available in [12]. It follows from Eqs. (97) and (98) that

$$\sigma(\delta_{QCD}) = [\sigma^2(\delta^0) + \sigma^2(\delta_{NP})]^{1/2} = 4\sigma(A_{\tau,v}^{exp.}), \quad (102)$$

where we have ignored the small correlation between $\delta^{(0)}$ and δ_{NP} . With the data provided by ALEPH [12], from Eqs. (98), (101) and (102) we obtain ¹⁴

$$\delta_{exp.}^{(0)} = 0.2091 \pm 0.0065_{exp.}, \quad (103)$$

it should be noted that in [14] slightly large value and error have been obtained, namely, $\delta_{exp.}^{(0)} = 0.2093 \pm 0.008_{exp.}$. The perturbative QCD correction obtained within CIPT is represented via the contour integral in the complex momentum squared plane [18,19]. This integral can be rewritten as

$$\delta_{CI}^{(0)} = \frac{1}{\pi} \int_0^\pi \text{Re} \left\{ (1 - e^{i\varphi}) (1 + e^{i\varphi})^3 d_{RGI}(s_0 e^{i\varphi}) \right\} d\varphi, \quad (104)$$

where $s_0 = m_\tau^2$ and $d_{RGI}(z)$ denote the RG improved perturbative correction to the Adler function defined in (14). To calculate $d_{RGI}(z)$, usually, the four loop order RG equation is solved numerically for the running coupling. We find convenient to use the implicit solution to the RG equation at the four loop order (relevant formulas can be found in [28]). The running coupling satisfies a transcendental equation which is solved numerically. To extract the value of the QCD scale parameter $\Lambda \equiv \Lambda_{\overline{\text{MS}}}$, one solves the equation

$$\delta_{CI}^{(0)}(\Lambda) = \delta_{exp.}^{(0)}. \quad (105)$$

Numerical values for the QCD scale parameter and strong coupling constant (for $n_f = 3$ number of flavours) extracted from the experimental value (103) are given in Table 11. We have used various approximations to the Adler function evaluated with the four loop running coupling. For the unknown N⁴LO coefficient of the Adler w_τ , we have used the geometric series estimate $d_5 \approx 378 \pm 378$ [14].

¹⁴ Alternatively, we could have determined the error on $\delta_{exp.}^{(0)}$ directly from the known error on $R_{\tau,V}$ using formula (96).

References

1. Bertlmann, R.A., Launer, G. and de Rafael, E.: Gaussian sum rules in quantum chromodynamics and local duality. Nucl. Phys. B250 (1985) 61.
2. de Rafael, E.: An Introduction to sum rules in QCD. Lectures at the Les Houches Summer School 1997. arXiv: 9802448 [hep-ph]
3. Peris, S., Perrottet, M., de Rafael, E.: Matching long and short distances in large- N_c QCD. JHEP **9805**, 011 (1998)
4. Shifman, M.A., Vainshtein, A.I., Zakharov, V.I.: QCD and resonance physics. Theoretical foundations. Nucl. Phys. B **147**, 385 (1979)
5. Poggio, E.C., Quinn, H.R., Weinberg, S.: Smearing method in the quark model. Phys. Rev.D **13** 1958-1968 (1976)
6. Braaten, E., Narison, S., and Pich, A.: QCD analysis of the tau hadronic width. Nucl. Phys. B **373**, 581 (1992)
7. Shifman, M.A.: Quark-hadron duality. Boris Ioffe Festschrift. At the Frontier of Particle Physics, Handbook of QCD, M. A. Shifman (ed.) World Scientific Singapore (2001)
8. Peris, S., Phily, B., de Rafael, E.: Tests of Large- N_c QCD from Hadronic τ Decay. Phys. Rev. Lett. **86**, 14-17 (2001)
9. Cata, O., Golterman, M., Peris, S.: Unraveling duality violations in hadronic tau decays. Phys. Rev. D **77**, 093006 (2008)
10. Cata, O., Golterman, M., Peris, S.: Possible duality violations in τ decay and their impact on the determination of α_s . Phys. Rev. D **79**, 053002 (2009)
11. Schael, S. et al.: Branching ratios and spectral functions of τ decays: Final ALEPH measurements and physics implications [ALEPH Collaboration]. Phys. Rept. **421**, 191 (2005)
12. The ALEPH data for the spectral functions is available at <http://aleph.web.lal.in2p3.fr/tau/specfun.html>.
13. Davier, M., Höcker, A., Zhang, Z.: The physics of hadronic tau decays. Rev. Mod. Phys. **78** 1043 (2006)
14. Davier, M., Höcker, A.H., Zhang, Z.: The determination of α_s from τ decays revisited. Eur. Phys. J. C **56**, 305-322 (2008)
15. Mason, Q. et al.: Accurate determinations of α_s from realistic lattice QCD. Phys. Rev. Lett. **95**052002 (2005)
16. Maltman, K., Yavin, T.: $\alpha_s(M_\tau^2)$ from hadronic τ decays. Phys. Rev. D **78** 094020 (2008)
17. Pivovarov, A.A.: Sov. J. Nucl. Phys. **54**, 676 (1991)
18. Pivovarov, A.A.: Renormalization group analysis of the τ -lepton decay within QCD. Z. Phys. C **53** 461-464 (1992) [hep-ph/0302003].
19. Le Diberger F., Pich A.: The perturbative QCD prediction to R_τ revisited. Phys. Lett. B **286**, 147-152 (1992)
20. Jamin, M.: Contour-improved versus fixed-order perturbation theory in hadronic tau decays. JHEP **0509**, 058 (2005)
21. Beneke, M., Jamin, M.: α_s and the τ hadronic width: fixed-order, contour-improved and higher-order perturbation theory. JHEP **0809**, 044 (2008)
22. Körner, J.G., Krajewski, F., Pivovarov, A.A.: Strong coupling constant from τ decay within a renormalization scheme invariant treatment. Phys. Rev. D **63**, 036001 (2003)
23. Kataev, A.L., Starshenko, V.V.: Estimates of the higher-order QCD corrections to $R(s)$, R_τ and deep inelastic scattering sum rules. Mod. Phys. Lett. A **10**, 235 (1995)
24. Raczka, P.A.: Towards more reliable perturbative QCD predictions at moderate energies. arXiv: hep-ph/0602085
25. Gardi, E., Grunberg, G., Karliner, M.: J. High Energy Phys. **07**, 007 (1998)
26. Magradze, B.A.: The gluon propagator in analytic perturbation theory. In: Proceedings of the 10th International Seminar "QUARKS-98" Suzdal, Russia, 1998 (Bezrukov F. L., et al.: eds.), vol 1, p. 158, Moscow: Russian Academy of Sciences, Institute for Nuclear Research 1999
27. Magradze, B.A.: An analytic approach to perturbative QCD. Int. J. Mod. Phys. A **15**, 2715 (2000)
28. Magradze, B.A.: A novel series solution to the renormalization group equation in QCD. Few-Body Systems **40**,71-99 (2006)
29. Krasnikov, A.N., Pivovarov, A.A.: Renormalization schemes and renormalons. Mod. Phys. Lett. A **11**, 835 (1996)
30. Shirkov, D.V., Solovtsov, I.L.: Analytic model for the QCD running coupling with universal $\bar{\alpha}_s(0)$ Value. Phys. Rev. Lett. **79**, 1209 (1997)

31. Dokshitzer, Yu., Marchesini, G., Webber, B.R.: Dispersive Approach to Power-Behaved Contributions in QCD Hard Processes. Nucl. Phys. B **469**, 93 (1996)
32. Grunberg, G.: On power corrections in the dispersive approach. JHEP **9811**, 006 (1998)
33. Milton, K.A., Solovtsov, I.L., Solovtsova, O.P.: Analytic perturbation theory and inclusive tau Decay. Phys. Lett. B **415**, 104 (1997)
34. Solovtsov, I.L., Shirkov, D.V.: Analytic approach in quantum chromodynamics. Theor. Math. Phys. **120**, 1220 (1999)
35. Shirkov, D.V.: Analytic perturbation theory in analyzing some QCD observables. Eur. Phys. J. C **22**, 331 (2001)
36. Shirkov, D.V., Solovtsov, I.L.: Ten years of the Analytic Perturbation Theory in QCD. Theor. Math. Phys. **150** 132-152 (2007)
37. Milton, K.A., Solovtsova, O.P.: Perturbative expansions in the inclusive decay of the tau lepton. Int. J. Mod. Phys. A **17**, 3789 (2002)
38. Milton, K.A., Solovtsov, I.L., O.P. Solovtsova, O.P.: The Adler Function for Light Quarks in Analytic Perturbation Theory. Phys. Rev. D **64** 016005 (2001)
39. Cvetič, G., Valenzuela, C., Schmidt, I.: A modification of minimal analytic QCD at low energies. arXiv: 0508101 [hep-ph]
40. Bakulev, A.P., Mikhailov, S.V., Stefanis, N.G.: QCD Analytic Perturbation Theory. From integer powers to any power of the running coupling. Phys. Rev. D **72**, 074014 (2005)
41. Prosperi, G.M., Raciti, M., Simolo, C.: On the running coupling constant in QCD. Prog. Part. Nucl. Phys. **58**, 387-438 (2007)
42. R. Barate et. al.: Measurement of the axial-vector τ spectral functions and determination of $\alpha_s(M_Z^2)$ [ALEPH Collaboration]. Eur. Phys. J. C **4**, 409-431 (1998)
43. K. Ackerstaff, K., et al. Measurements of the strong coupling constant α_s and the vector and axial vector spectral functions in hadronic tau decays. [OPAL Collaboration] Eur. Phys. J. C **7**, 571 (1999)
44. Eidelman, S., Jagerlehner, F., Kataev, A.L., Veretin O.: Testing non-perturbative strong interaction effects via the Adler function. Phys. Lett. B **454**, 369-380 (1999)
45. Chetyrkin, K.G., Kataev, A.L., Tkachov F.V.: Higher Order Corrections to $\sigma_t(e^+ + e^- \rightarrow \text{Hadrons})$ in Quantum Chromodynamics. Phys. Lett. B **85**, 277 (1979)
46. Gorishnii, S.G., Kataev, A.L., Larin, S.A.: The $O(\alpha_s^3)$ corrections to $\sigma_{tot}(e + e^- \rightarrow \text{hadrons})$ and $\Gamma(\tau \rightarrow \text{tau-neutrino} + \text{hadrons})$ in QCD. Phys. Lett. B **259** 144-150 (1991)
47. Surguladze L.R., Samuel, M.A.: Total hadronic cross-section in $e^+ e^-$ annihilation at the four loop level of perturbative QCD. Phys. Rev. Lett. **66** 560-563 (1991) (1991 Erratum-ibid. **66**, 2416 (1991))
48. Baikov, P.A., Chetyrkin, K.G., Kühn, J.H.: Hadronic Z- and tau-Decays in Order α_s^4 . Phys. Rev. Lett. **101** 012002, (2008)
49. Chetyrkin, K.G., Kühn, J.H., Kwiatkowski, A.: QCD corrections to the e^+e^- cross-section and the Z boson decay rate: concepts and results. Phys. Rep. **277** 189-281 (1996)
50. Kourashev, D.S.: The QCD observables expansion over the scheme-independent two-loop coupling constant powers, the scheme dependence reduction. arXiv: 9912410 [hep-ph]
51. Kourashev, D.S., Magradze, B.A.: Explicit expressions for Euclidean and Minkowskian QCD observables in analytic perturbation theory. Theor. Math. Phys. **135**, 531 (2003)
52. Rodrigo, G., Santamaria, A.: QCD Matching Conditions at Thresholds. Phys. Lett. B **313** 441-446 (1993)
53. Chetyrkin, K.G., Kniehl, B.A., Steinhauser, M.: Strong Coupling Constant with Flavour Thresholds at Four Loops in the $\overline{\text{MS}}$ Scheme. Phys. Rev. Lett. **79** 2184-2187 (1997)
54. Rodrigo, G., Pich A., Santamaria A.: $\alpha_s(m_Z)$ from tau decays with matching conditions at three loops. Phys. Lett. B **424** 367-374 (1998)
55. Particle Data Group, Yao, W.M. et al.: J. Phys. G **33**,1 (2006) and 2007 partial update for the 2008 edition
56. Hudson, D.J.: STATISTICS, Lectures on Elementary Statistics and Probability. Geneva 1964.
57. Van Ritberger, T., Vermaseren, J.A.M., Larin, S.A.: The four-loop β -function in Quantum Chromodynamics. Phys. Lett B **400**, 379 (1997)
58. Corless, R.M., et al.: On the Lambert W function. Advances in Computation Mathematics **5**, 329 (1996).